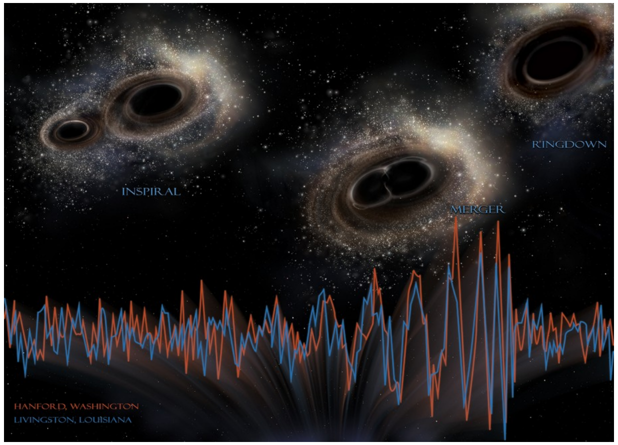

Searching for the Stochastic Gravitational-Wave Background with Advanced LIGO and Advanced Virgo

Nelson Christensen (for the LIGO Scientific Collaboration and the Virgo Collaboration)
Artemis, Observatoire de la Côte d’Azur, Nice

June 1, 2017. GWPAW 2017. G1700956

Talk Outline

- Review of Advanced LIGO Observing Run 1 Observations
- Implications of the first LIGO detections on the background from BBHs
- LIGO-Virgo data analysis methods for a stochastic gravitational wave background
- O1 stochastic analysis and preliminary results
- Non-standard GR stochastic searches
- Future Advanced LIGO – Advanced Virgo Observing Runs, O2 Update
- Conclusions

Stochastic Gravitational-wave Background

- Incoherent superposition of many unresolved sources.
- Cosmological:
  - » Inflationary epoch, preheating, reheating
  - » Phase transitions
  - » Cosmic strings
  - » Alternative cosmologies
- Astrophysical:
  - » Supernovae
  - » Magnetars
  - » Binary black holes
- Potentially could probe physics of the very-early Universe.

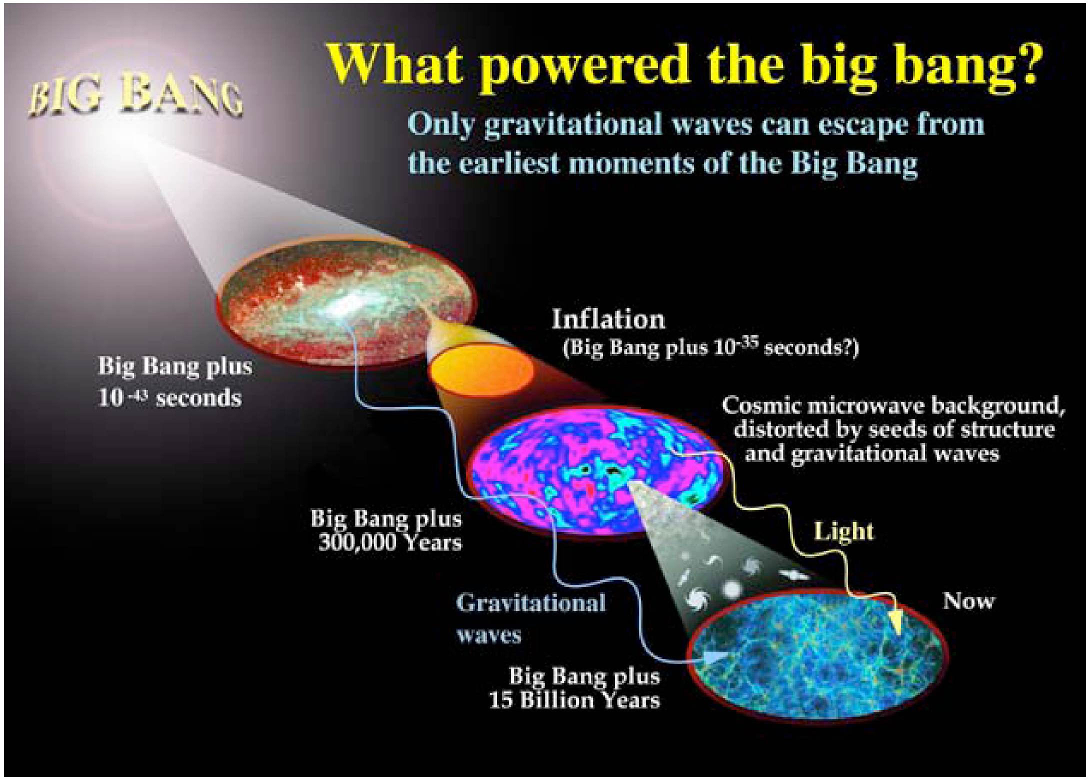

$$\Omega_{GW}(f) = \frac{f}{\rho_c}\frac{d\rho_{GW}}{df} \qquad \Omega_{GW}(f) = A(f/f_{ref})^{\alpha}$$

O1 Binary Black Hole Events

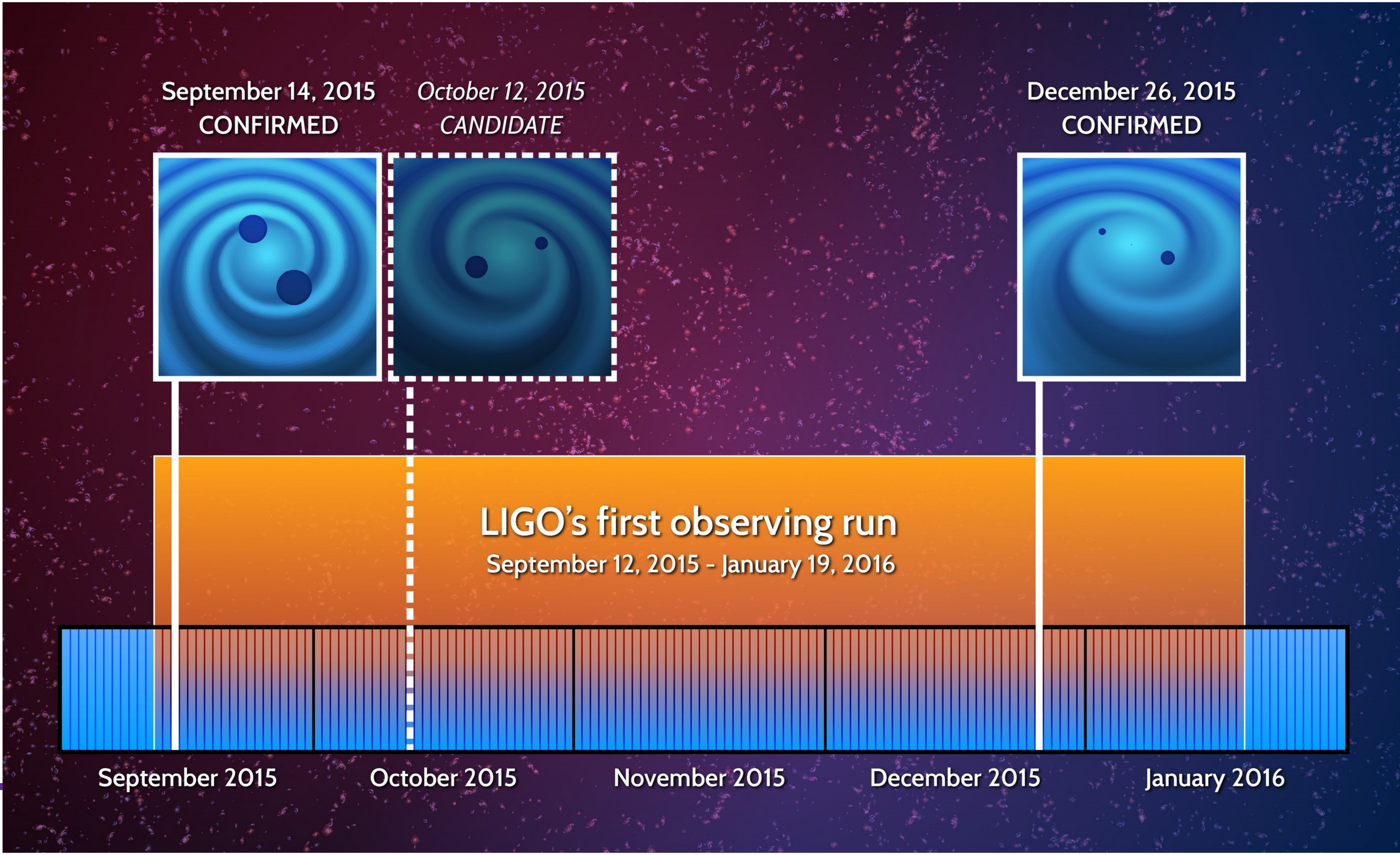

Image Credit - LIGO

Implications of LIGO first detections

- On Sept 14th 2015 LIGO detected for the first time the GW signal from a stellar binary black hole (BBH) at z~0.1 (GW150914). *PhysRevLetter.116.061102*

- Another event (GW151226), and likely a third (LVT151012), were detected in the LIGO first observational run. *PRX 6, 041015 (2016).*

- Besides the detection of loud individual sources at close distances, we expect to see the background formed by all the sources from the whole Universe (up to z~20)

- GW150914 told us that black hole masses ($m_{1,2}$~$30M_o$) can be larger than previously expected.

- Revised previous predictions of the GW background from BBHs, assuming various formation scenarios. *PhysRevLetter.116.131102*

Binary Black Hole Merger Rate

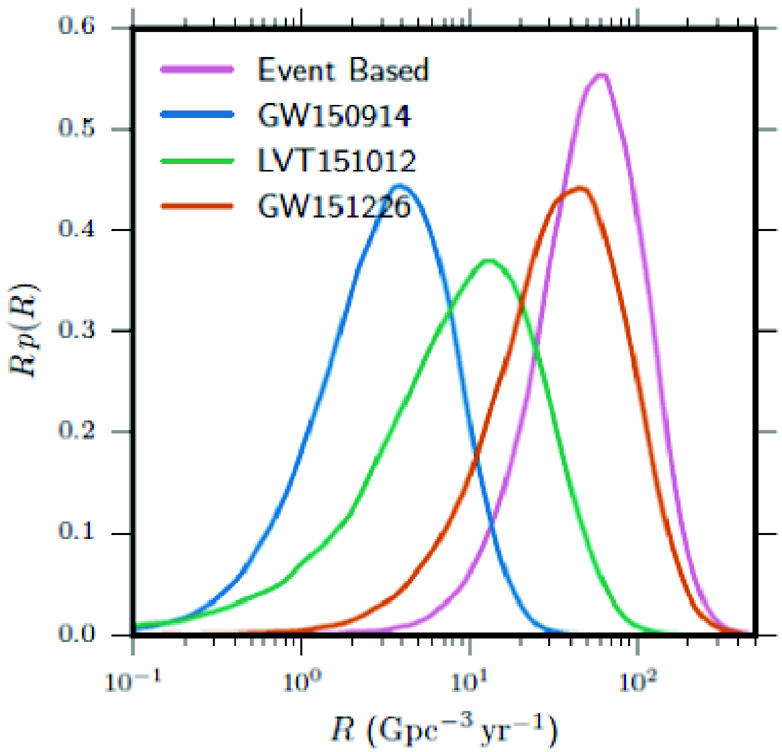

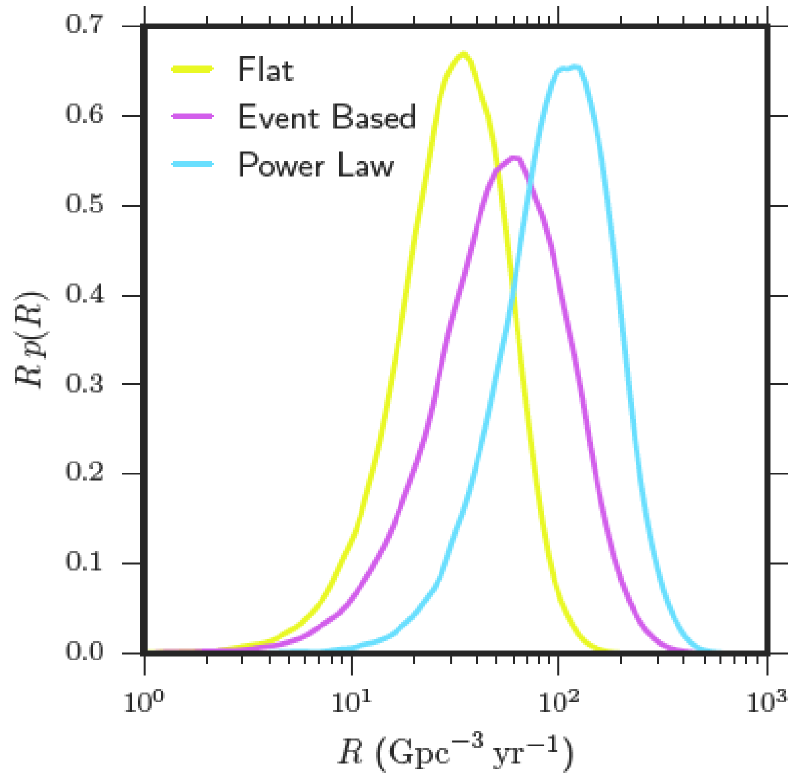

90% allowed range: [9-240] /Gpc^3/yr

PHYSICAL REVIEW X 6,041015 (2016)

Astrophysics: Binary Formation

- Two binary formation mechanisms have been proposed.
- Field:
  - » Starting from a binary star system, with each star going through the core-collapse to a black hole.

- Dynamic:
  - » Individually formed black holes in dense environments (globular clusters) fall toward the center of the potential well, where they dynamically form binaries (and are often ejected).

Implications for a Stochastic Background of GWs

• For every detected binary merger, there are many more that are too distant and too faint.

• They generate a stochastic background of gravitational waves.

$$\Omega_{\rm GW}(f;\theta_k) = \frac{f}{\rho_c H_0} \int_0^{z_{\max}} dz \frac{\underbrace{R_m(z,\theta_k)}_{\text{Merger Rate}} \underbrace{\frac{dE_{\rm GW}}{df_s}(f_s,\theta_k)}_{\text{Source Energy Spectrum}}}{(1+z)\underbrace{E(\Omega_{\rm M},\Omega_\Lambda,z)}_{\text{Cosmology}}}$$

• Relatively high rate and large masses of observed systems implies a relatively strong stochastic background.

Implications for a Stochastic Background of GWs

Probing compact binary decays predominantly between z ~ 1 – 3.

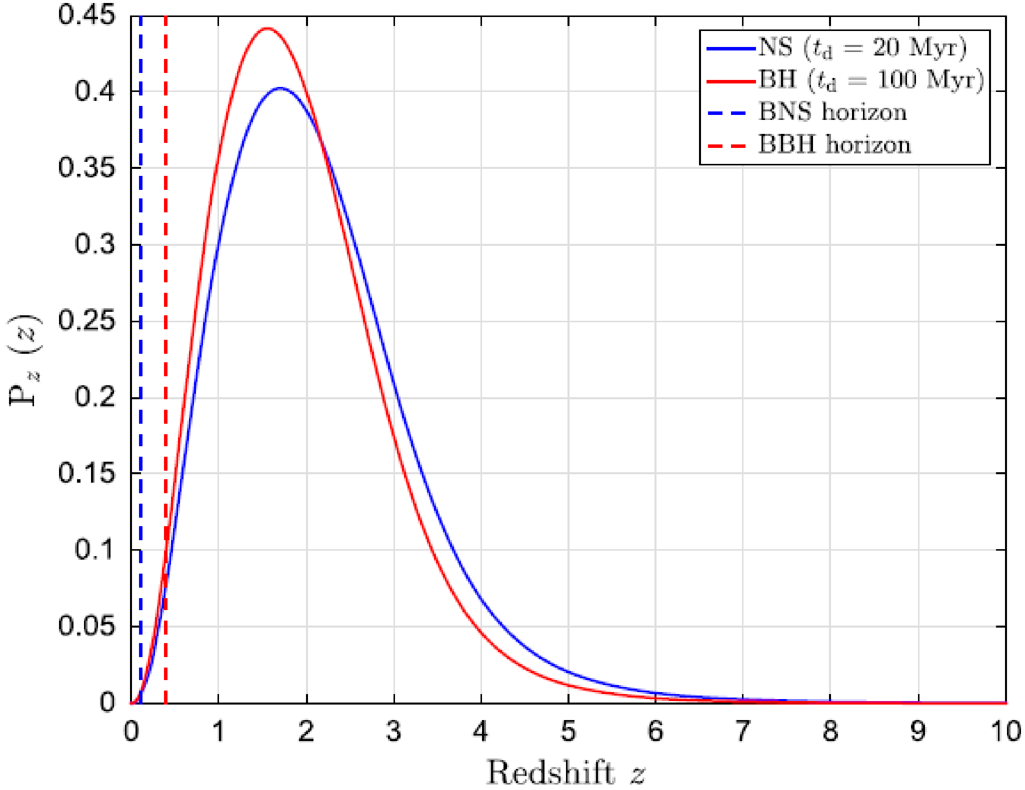

Source redshift probability distribution for binary neutron stars and (blue) and binary black holes (red).

PHYSICAL REVIEW D 92,063002 (2015)

Implications for a Stochastic Background of GWs

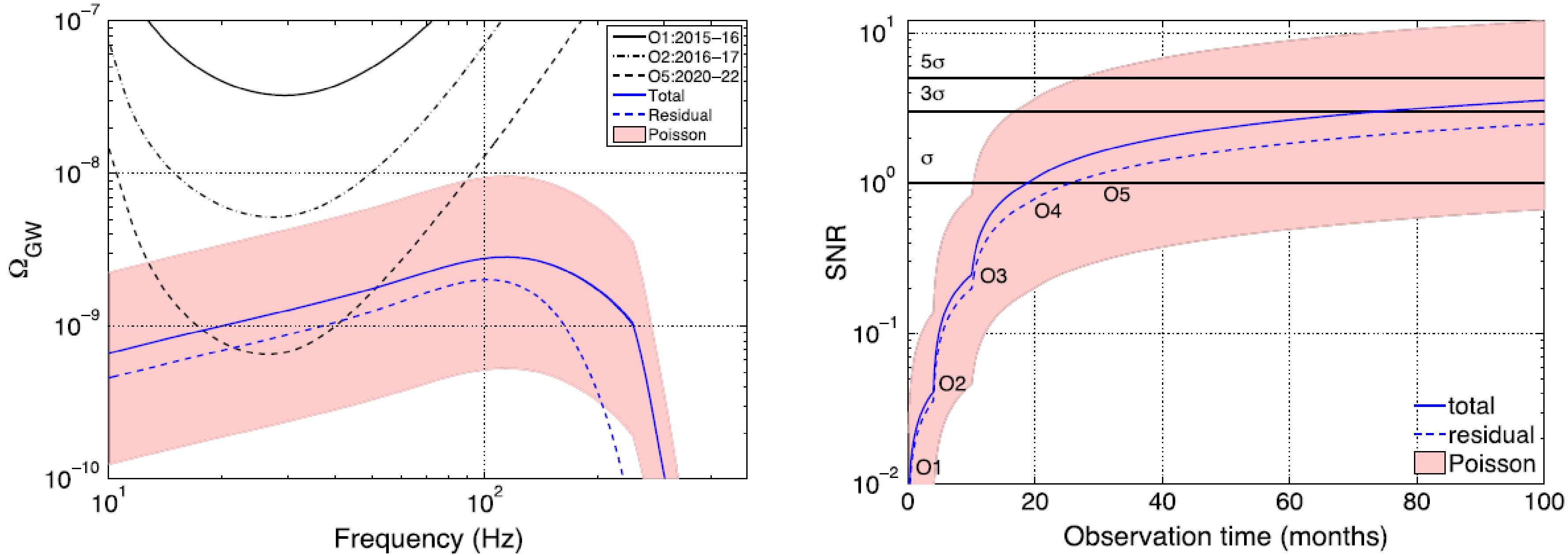

Based on the Field formation mechanism, assuming GW150914 parameters.

Assumptions are necessary; best information available in literature.

Abbott et all (LIGO-Virgo) Physical Review Letters **116**, 131102 (2016)

Alternative Models

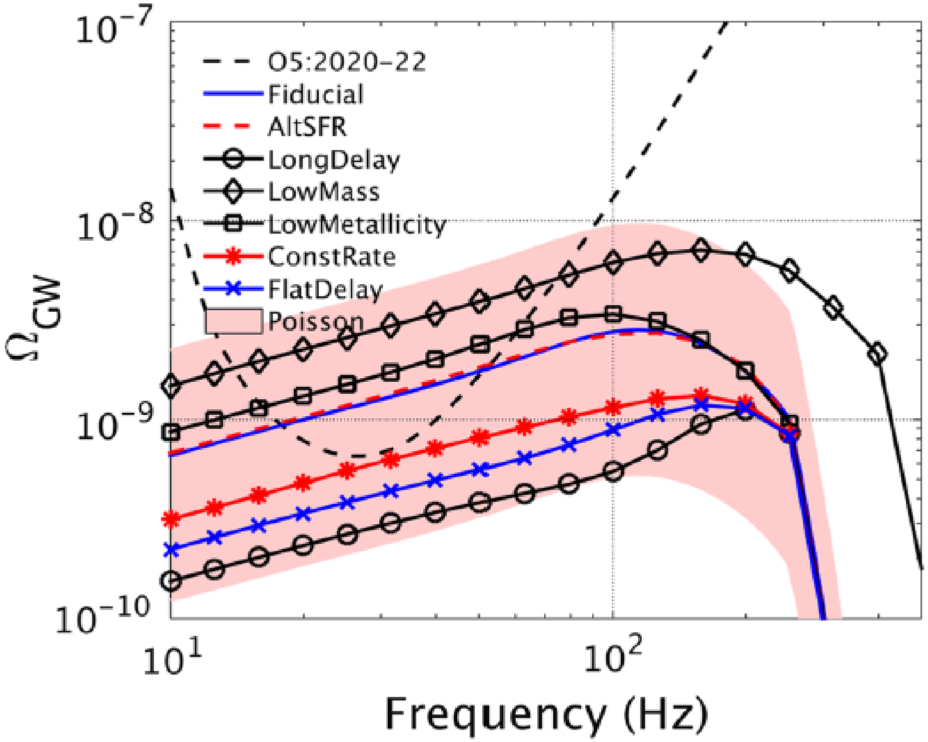

- Model variations imply relatively small changes in the energy spectrum.
- Large Poisson statistical uncertainty.
- Dominated by z ~1-2 contributions.
- Conservative estimates.
- A foreground to cosmological models of stochastic background.

Abbott et all (LIGO-Virgo) Physical Review Letters **116**, 131102 (2016)

Implications for a Stochastic Background of GWs

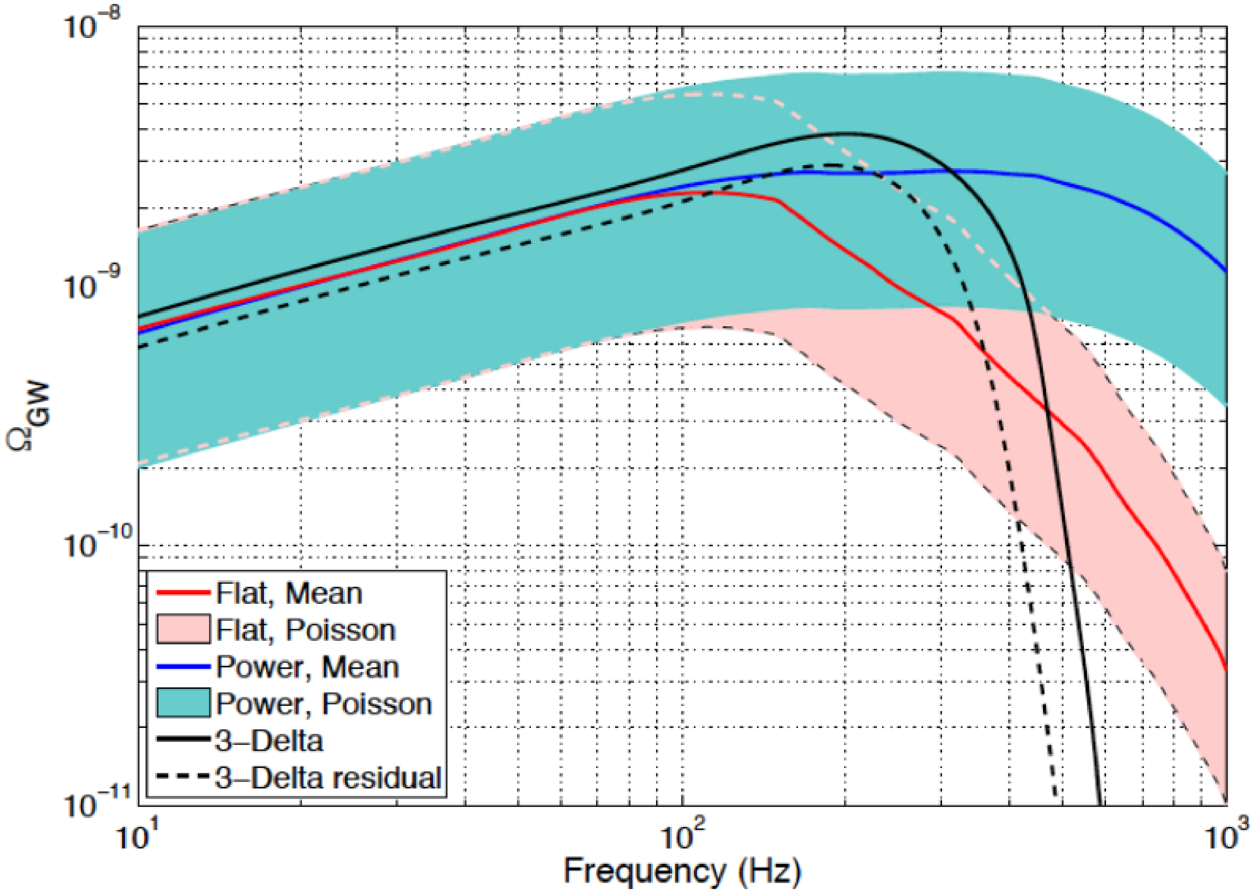

All of O1.

3 events.

Same mean value Ω_{gw} (25 Hz)~ 10^{-9}

Less uncertainty

Abbott et all (LIGO-Virgo), Phys. Rev. X 6, 041015 (2016)

There is a good chance that LIGO-Virgo will observe this BBH produced stochastic background in the next 3 to 5 years.

Gravitational wave background from Population III binary black holes consistent with cosmic reionization

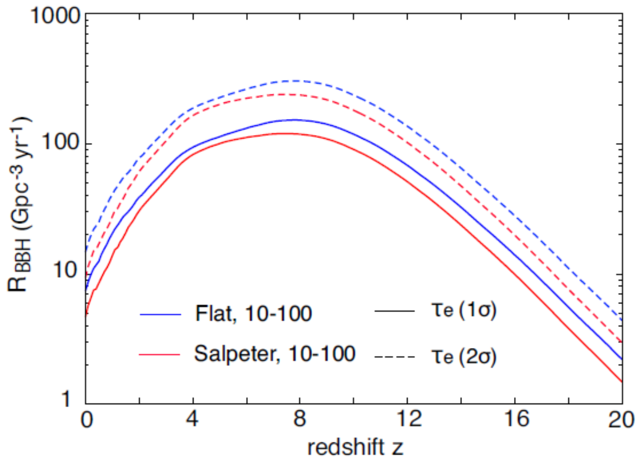

Figure 3. Merger rate of PopIII BBHs for different assumed IMFs, as in Fig. 2. The data is taken from K14, but renormalized to be consistent with the electrons scattering optical depth τ_e measured by *Planck* within the 1σ (solid) and 2σ (dashed) error (Eq. 1 with $f_{\rm esc,m} = 0.1$ and $\eta_{\rm ion} = 5 \times 10^4$).

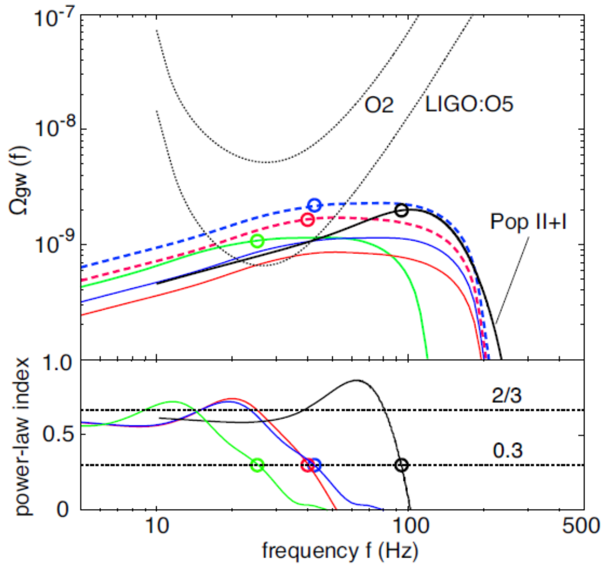

Figure 4. *Top*: spectra of GWB produced by PopIII BBHs for the same IMFs, $f_{\rm esc,m}$ and τ_e as in Fig. 3 (blue and red curves). We assume binaries with the average chirp mass of $\langle M_{\rm chirp}\rangle = 30\ {\rm M}_\odot$ on circular orbits. The background expected from all unresolved PopII+PopI BBHs is shown for reference (solid black curve, Abbott et al. 2016b, their fiducial model). Black dotted curves show the expected sensitivity of AdLIGO/Virgo in the observing runs O2 and O5. The green solid curve is the same as the blue solid curve, but with a higher chirp mass of $\langle M_{\rm chirp}\rangle = 50\ {\rm M}_\odot$ and with a lower merging rate by a factor of 3/5. *Bottom*: the spectral index; open circles mark the frequencies above which $\alpha < 0.3$.

Potentially a stronger stochastic background than what we would expect from direct BBH observations.

K. Inayoshi et al., Mon Not R Astron Soc (2016) 461 (3): 2722-2727.

Did LIGO Detect Dark Matter?

- "There remains a window for masses $20\ M_\odot \lesssim M_{bh} \lesssim 100\ M_\odot$ where primordial black holes (PBHs) may constitute the dark matter."
- Reasonable rate estimates overlap LIGO rate limits.
- No neutrino or optical counterparts.
- "They may be distinguished from mergers of BHs from more traditional astrophysical sources through the observed mass spectrum, their high ellipticities, or their stochastic gravitational wave background." S. Bird et al., PRL 116, 201301 (2016)
- "We show that if PBHs make up the dark matter, then roughly one event should have a detectable eccentricity given LIGO's expected sensitivity and observing time of six years." I. Cholis et al., PRD 94, 084013 (2016)

Stochastic Background – Primordial Black Hole

"We have shown that the amplitude of this spectrum is significantly lower than that arising from the stellar BBH mergers, although there is currently a large uncertainty in the local merger rate for stellar BBH systems.

…

Consequently, the stochastic GW background measurement with Advanced LIGO detectors is unlikely to detect this background."

Other studies are more optimistic:

https://arxiv.org/abs/1610.08725
https://arxiv.org/abs/1610.08479

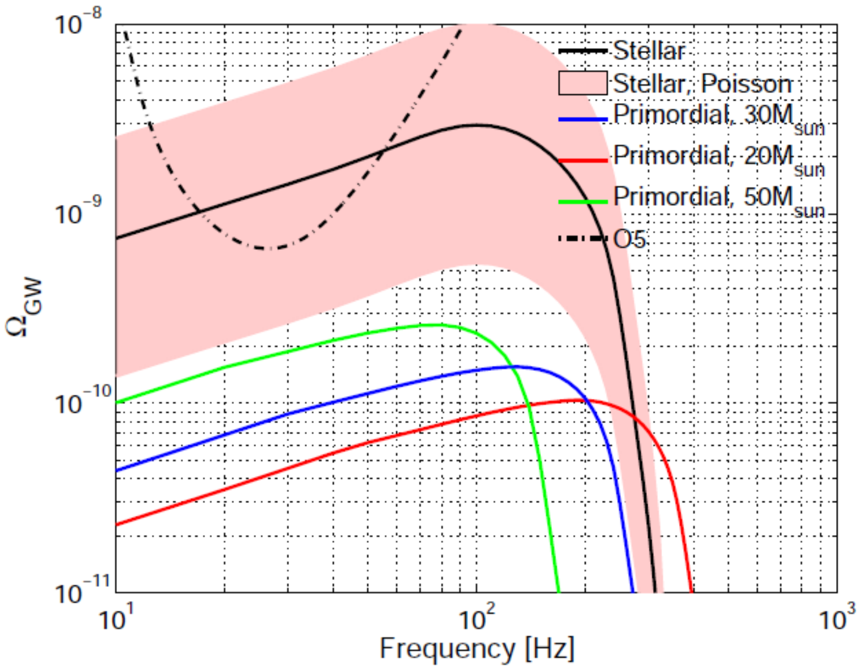

FIG. 4: Gravitational-wave energy density for the primordial BBH model is shown as a function of frequency for several values of the black hole mass, assuming the Ludlow et al. concentration model [28] and the Watson et al. model of the halo mass function [31]. Also shown is the projected final sensitivity of advanced detectors, denoted O5, as well as the fiducial stellar model and its Poisson error band [34].

V. Mandic et al., Phys. Rev. Lett. **117**, 201102 (2016)

Data Analysis

- Assume stationary, unpolarized, isotropic and Gaussian stochastic background
- Cross correlate the output of detector pairs to eliminate the noise

$$s_i = h_i + n_i$$

$$< s_1 s_2 > = < h_1 h_2 > + \underbrace{< n_1 n_2 >}_{0} + \underbrace{< h_1 n_2 >}_{0} + \underbrace{< n_1 h_2 >}_{0}$$

Isotropic search

- Frequency domain cross product:

$$Y = \int \tilde{s}_1^*(f)\tilde{Q}(f)\tilde{s}_2(f)df$$

- optimal filter:

$$\tilde{Q}(f) \propto \frac{\gamma(f)\Omega_{gw}(f)}{f^3 P_1(f) P_2(f)} \text{ with } \Omega_{gw}(f) \equiv \Omega_\alpha f^\alpha$$

- in the limit noise >>GW signal

$$\text{Mean}(Y) = \Omega_0 T,\ \text{Var}(Y) \equiv \sigma^2\ \mu\ T,\ \text{SNR}\ \mu \sqrt{T}$$

Overlap reduction function

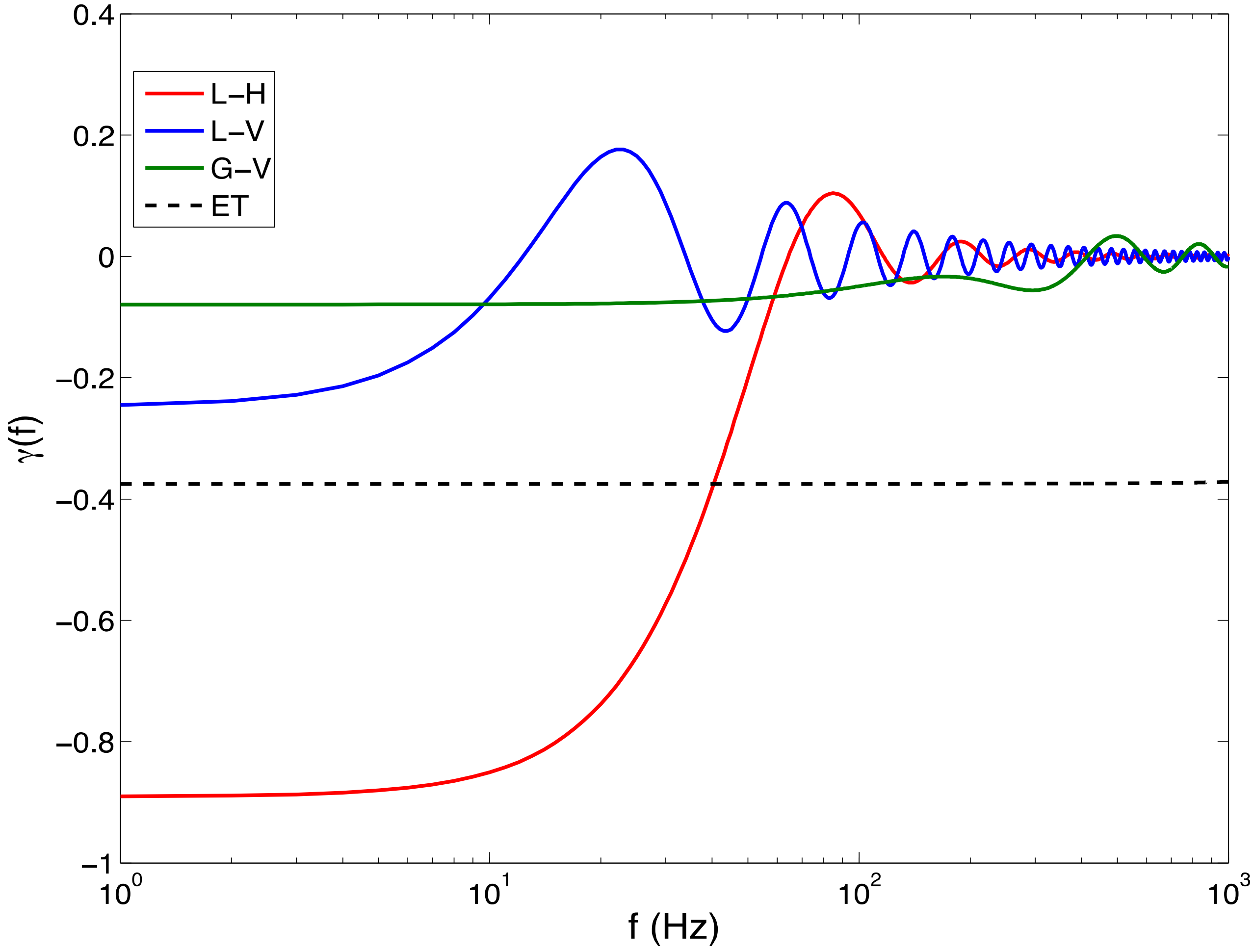

O1 Stochastic Search Results

- No evidence for a stochastic background for both the isotropic and direction searches
- Put upper limits on the energy density for different power indices
- Took a long time to clean the data.
- For α=0, the isotropic bound is 33x better than with initial LIGO/Virgo

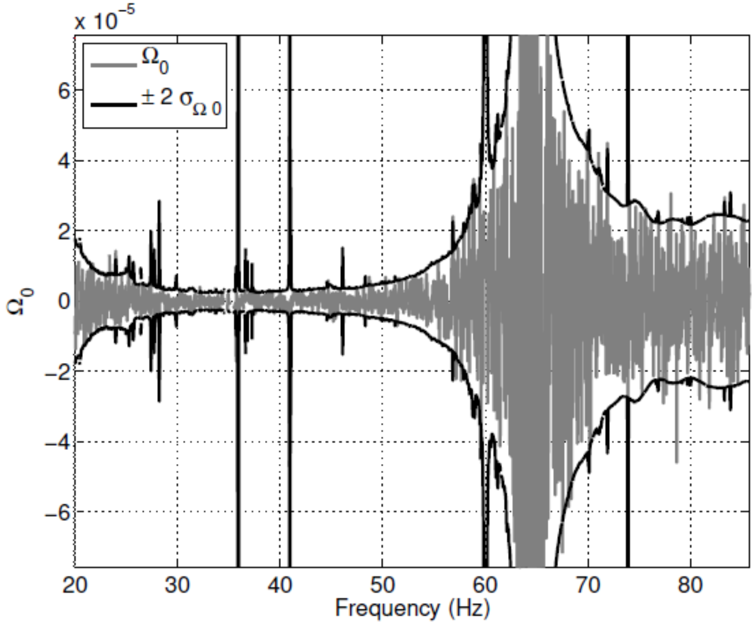

$$\Omega_{gw}(25\text{Hz}) < 1.7 \times 10^{-7}$$

(LSC-Virgo) PRL.118.121101 (2017)

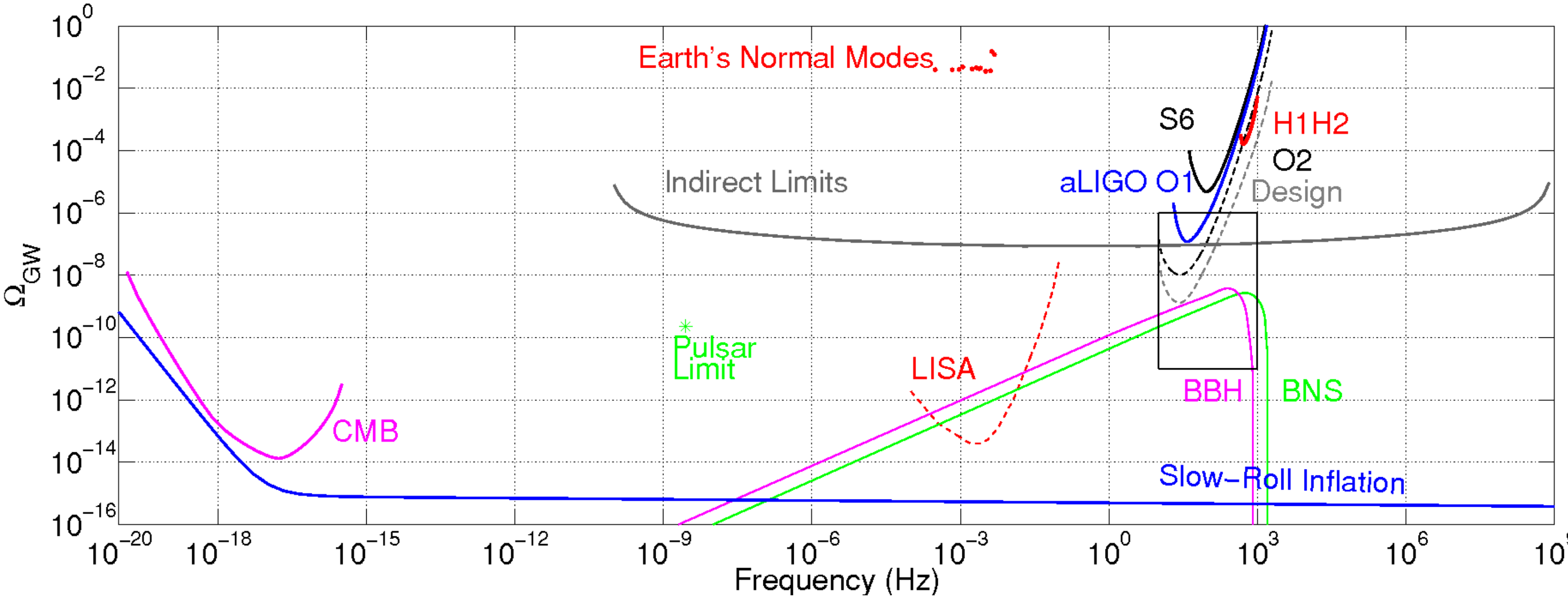

Indirect limits: P. Lasky et al., PhysRevX.6.011035 (2016)
"CMB temperature and polarization power spectra, lensing, BAOs and BBN"

PI integrated sensitivity curves: E. Thrane & J. Romano PhysRevD.88.124032 (2013)
"The LISA sensitivity curve corresponds to an autocorrelation measurement in a single detector assuming perfect subtraction of instrumental noise and/or any unwanted astrophysical foreground."

(LSC-Virgo) PRL.118.121101 (2017)

Spectral index α	Frequency band with 99% sensitivity	Amplitude Ω_α	95% CL upper limit	Previous limits [36]
0	20 – 85.8 Hz	$(4.4 \pm 5.9) \times 10^{-8}$	1.7×10^{-7}	5.6×10^{-6}
2/3	20 – 98.2 Hz	$(3.5 \pm 4.4) \times 10^{-8}$	1.3×10^{-7}	–
3	20 – 305 Hz	$(3.7 \pm 6.5) \times 10^{-9}$	1.7×10^{-8}	7.6×10^{-8}

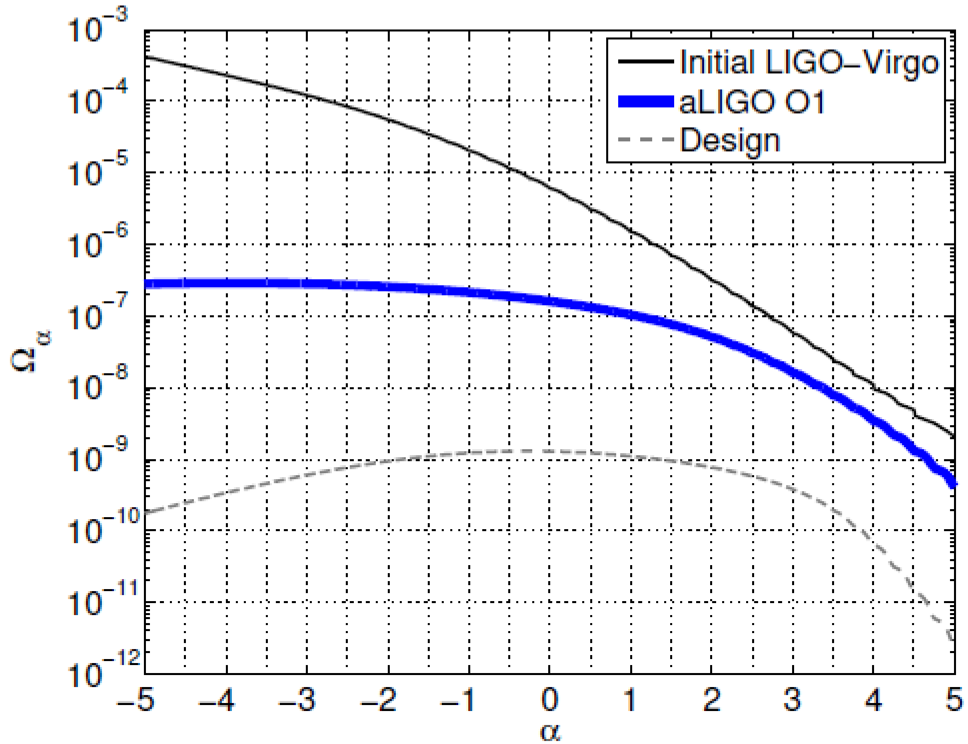

FIG. 2. Following [52], we present 95 % confidence contours in the $\Omega_\alpha - \alpha$ plane. The region above these curves is excluded at 95% confidence. We show the constraints coming from the final science run of Initial LIGO-Virgo [36] and from O1 data. Finally, we display the projected (not observed) design sensitivity to Ω_α and α for Advanced LIGO and Virgo [54].

(LSC-Virgo) PRL.118.121101 (2017)

Directional searches

- Relax assumption of isotropy and generalize the search for a stochastic signal to the case of arbitrary angular distribution.

$$\Omega_{\rm GW}(f) \equiv \frac{f}{\rho_c}\frac{d\rho_{\rm GW}}{df} = \frac{2\pi^2}{3H_0^2} f^3 H(f) \int_{S^2} d\hat{\Omega}\, \mathcal{P}(\hat{\Omega})$$

$$\boxed{\mathcal{P}(\hat{\Omega}) = \mathcal{P}_\alpha \mathbf{e}_\alpha(\hat{\Omega})}$$

Radiometer Analysis

Spherical Harmonic Decomposition

$$\mathcal{P}(\hat{\Omega}) \equiv \eta(\hat{\Omega}_0)\delta^2(\hat{\Omega}, \hat{\Omega}_0)$$

$$\mathcal{P}(\hat{\Omega}) \equiv \sum_{lm} \mathcal{P}_{lm} Y_{lm}(\hat{\Omega})$$

O1 Directional – Extended Sources

Spherical Harmonics (SHD)

All-sky (broadband) Results

						Max SNR (% p-value)		Upper limit range	
α	$\Omega_{\rm gw}$	$H(f)$	f_α (Hz)	θ (deg)	$l_{\rm max}$	BBR	SHD	BBR ($\times 10^{-8}$)	SHD ($\times 10^{-8}$)
0	constant	$\propto f^{-3}$	52.50	55	3	3.32 (7)	2.69 (18)	10 – 56	2.5 – 7.6
2/3	$\propto f^{2/3}$	$\propto f^{-7/3}$	65.75	44	4	3.31 (12)	3.06 (11)	5.1 – 33	2.0 – 5.9
3	$\propto f^{3}$	constant	256.50	11	16	3.43 (47)	3.86 (11)	0.1 – 0.9	0.4 – 2.8

SNR maps

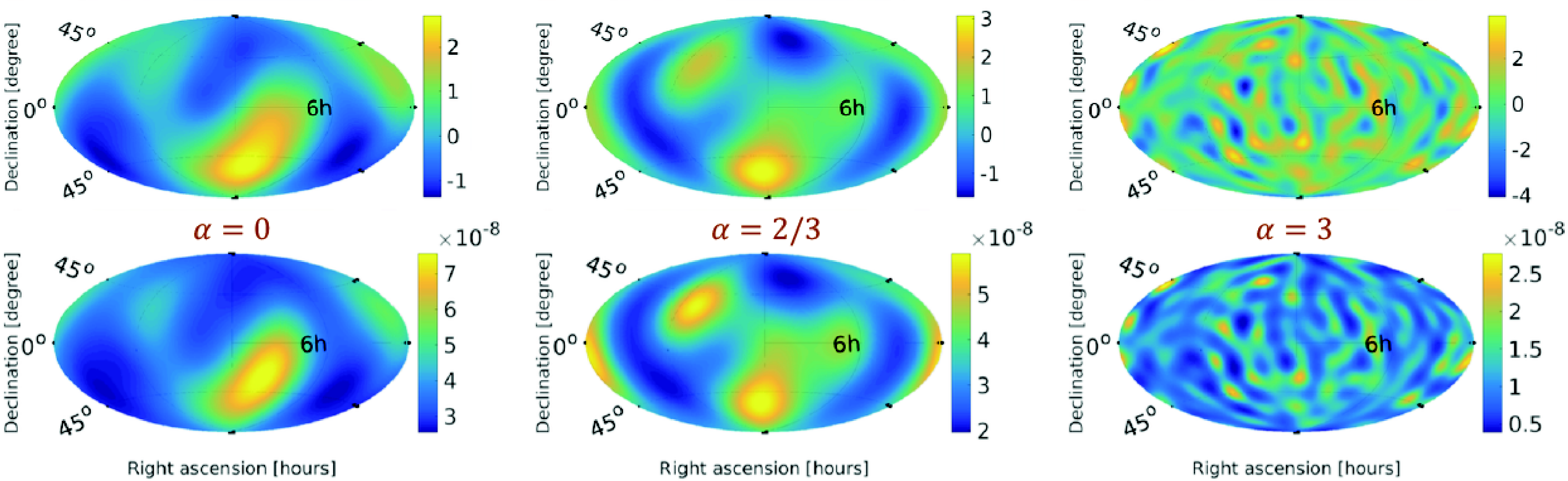

Upper Limit maps [$\Omega_{\rm gw}$ sr^{-1}]

(LSC-Virgo) PRL.118.121102 (2017)

O1 Directional – Point Sources

Broadband Radiometer (BBR)

All-sky (broadband) Results

α	$\Omega_{\rm gw}$	$H(f)$	f_α (Hz)	θ (deg)	$l_{\rm max}$	Max SNR (% p-value) BBR	Max SNR (% p-value) SHD	Upper limit range BBR ($\times 10^{-8}$)	Upper limit range SHD ($\times 10^{-8}$)
0	constant	$\propto f^{-3}$	52.50	55	3	3.32 (7)	2.69 (18)	10 – 56	2.5 – 7.6
2/3	$\propto f^{2/3}$	$\propto f^{-7/3}$	65.75	44	4	3.31 (12)	3.06 (11)	5.1 – 33	2.0 – 5.9
3	$\propto f^{3}$	constant	256.50	11	16	3.43 (47)	3.86 (11)	0.1 – 0.9	0.4 – 2.8

SNR maps

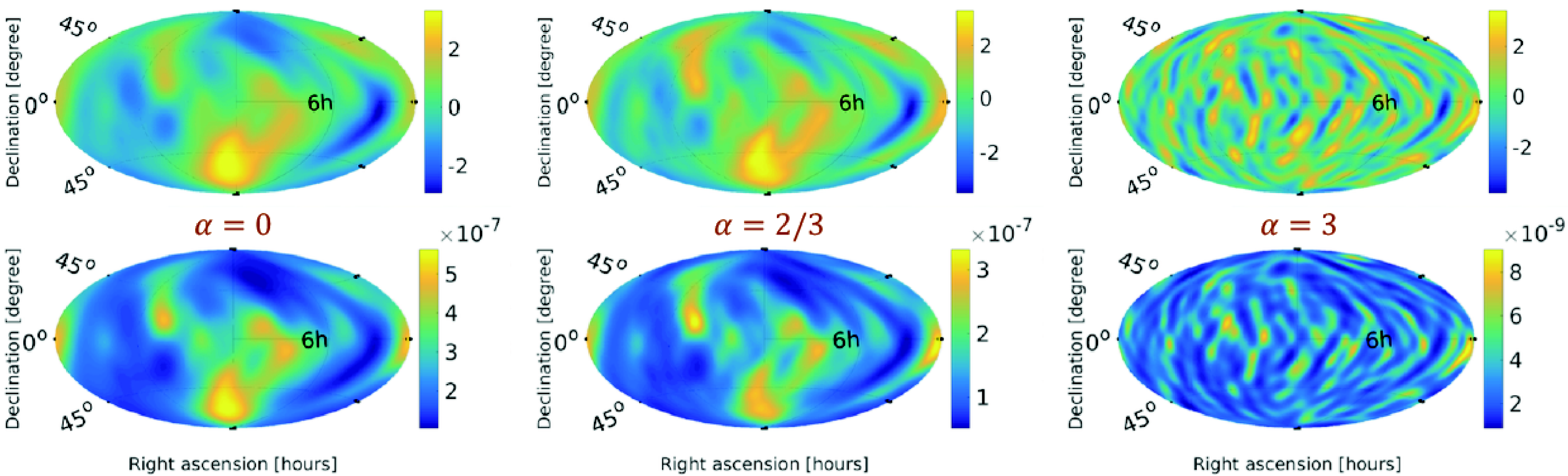

Upper Limit maps [erg cm^{-2} s^{-2} Hz^{-1}]

(LSC-Virgo)
PRL.118.121102 (2017)

O1 Directional – Directed

Narrowband radiometer

Results showing 90% upper limits on strain as a function of frequency for O1

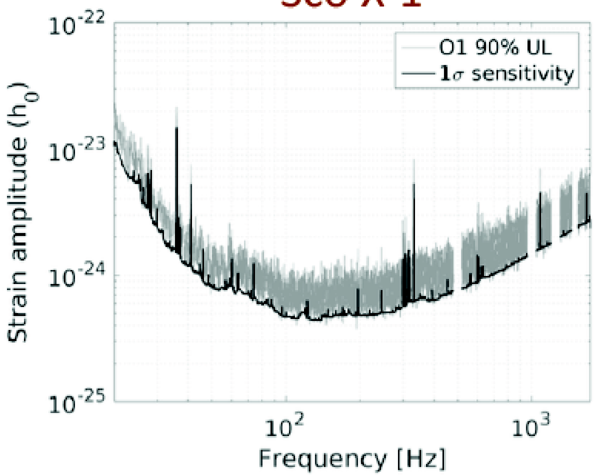

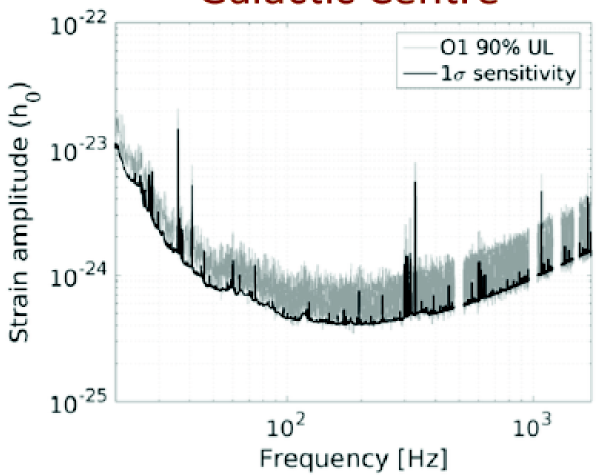

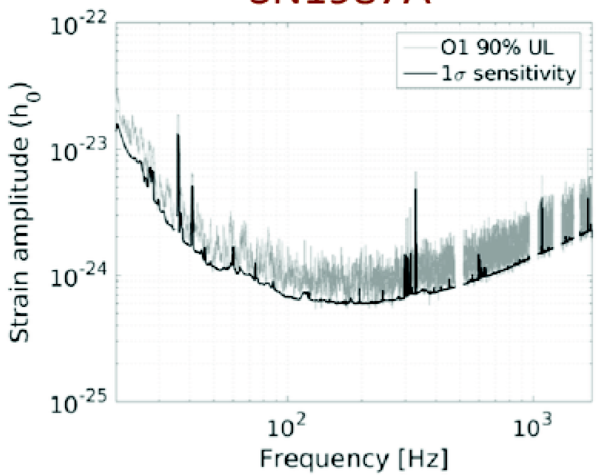

Narrowband Radiometer Results

Direction	Max SNR	p-value (%)	Frequency band (Hz)	Best UL ($\times 10^{-25}$)	Frequency band (Hz)
Sco X-1	4.58	10	616 – 617	6.7	134 – 135
SN1987A	4.07	63	195 – 196	5.5	172 – 173
Galactic Center	3.92	87	1347 – 1348	7.0	172 – 173

PRL.118.121102 (2017)

Correlated Magnetic Noise from the Schumann Resonances

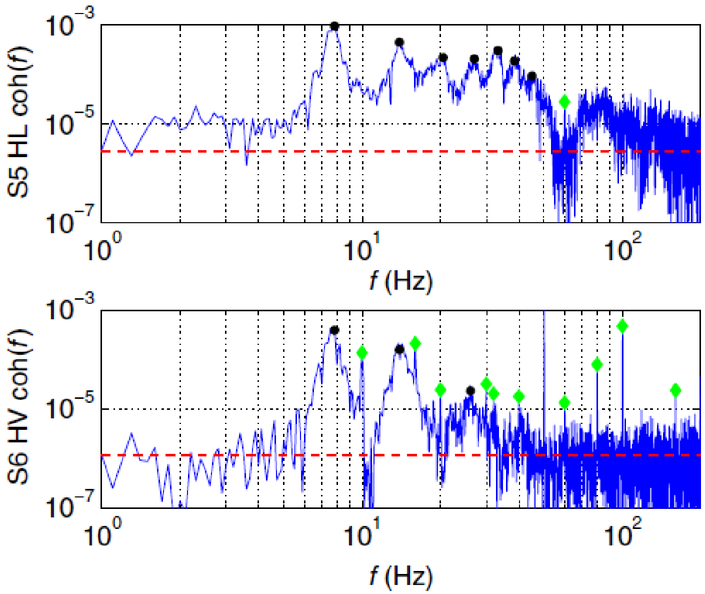

FIG. 1 (color online). Magnetometer coherence spectra for LHO-LLO during the LIGO S5 science run (top, $t_{\mathrm{obs}} =$ 330 dy) and for LHO-Virgo during S6-VSR2/3 (bottom, $t_{\mathrm{obs}} =$ 100 dy). Schumann resonance peaks are indicated with black circles while electronic noise lines are indicated with green diamonds. The red dashed line indicates the average value expected for uncorrelated noise. Some LHO-LLO peaks are obscured by 60 Hz electronic noise. The frequency resolution is 0.1 Hz.

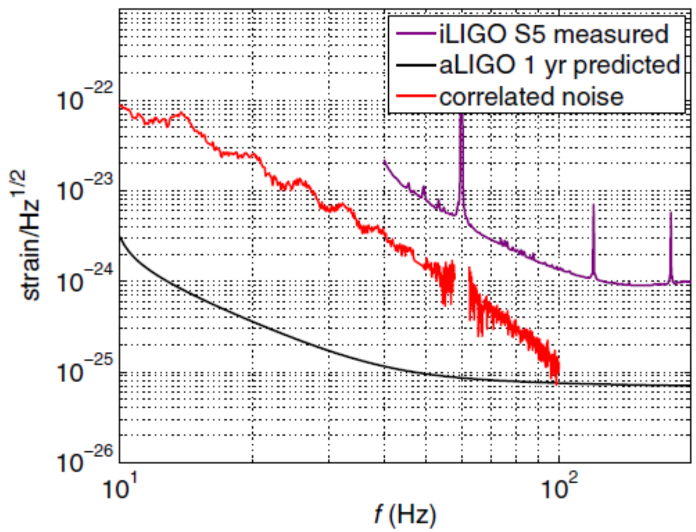

FIG. 3 (color online). Strain amplitude spectra for correlated and uncorrelated noise. Black is the uncorrelated noise $\sqrt{N_{12}^{\mathrm{u}}(f)}$ for the H1L1 detector pair operating at Advanced LIGO design sensitivity and assuming 1 yr of integration. Purple indicates the uncorrelated noise $\sqrt{N_{12}^{\mathrm{u}}(f)}$ achieved during initial LIGO using $\approx$300 days of coincident data. Red is $\sqrt{N_{12}^{\mathrm{m}}(f)}$ (the estimated correlated noise due to EM fields during initial LIGO). Electronic noise lines have been notched. The spectra have been scaled to assume a frequency resolution of 0.25 Hz, which is typical for stochastic searches [26].

Monitor correlated magnetic noise level in O1 and future runs. E. Thrane et al., PRD **87**, 123009 (2013)

Magnetometer Coherence Virgo - KAGRA

Fun Fact: The Schumann signal is actually a bit stronger underground than above ground at KAGRA.

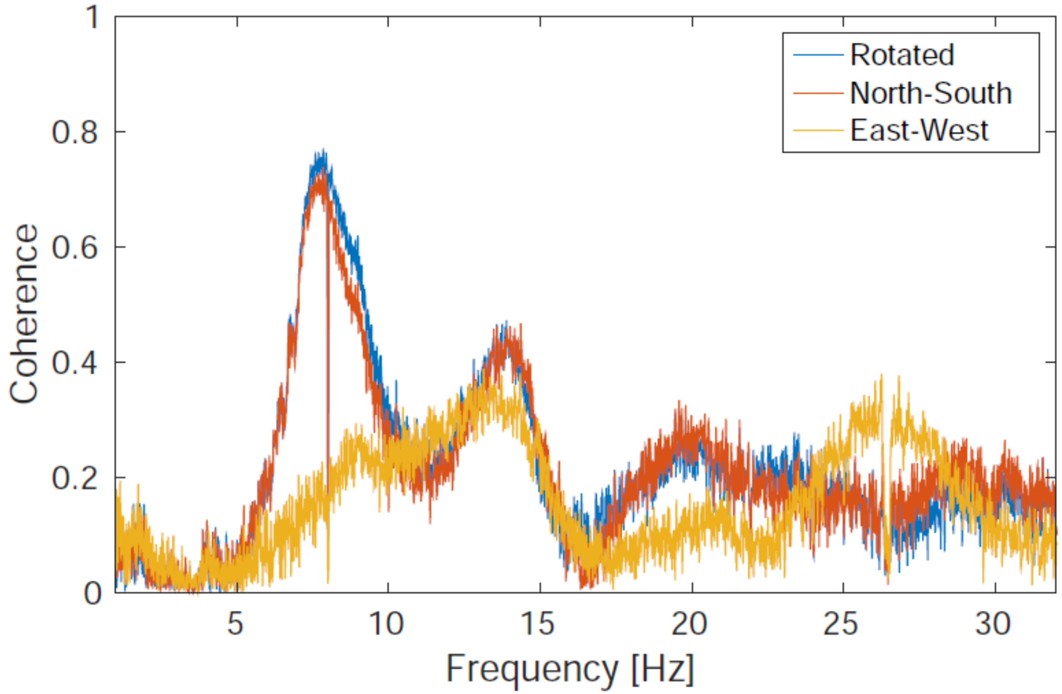

(c) Coherence Max

There is the possibility that the global magnetic fields could limit the ability of LIGO-Virgo-KAGRA to limit or measure the stochastic background.

Wiener Filtering – Low noise magnetometers at the sites.
Studies on-going with many researchers from LIGO, Virgo and KAGRA.

Correlated Transient Magnetic Noise – The Source of the Schumann Resonances

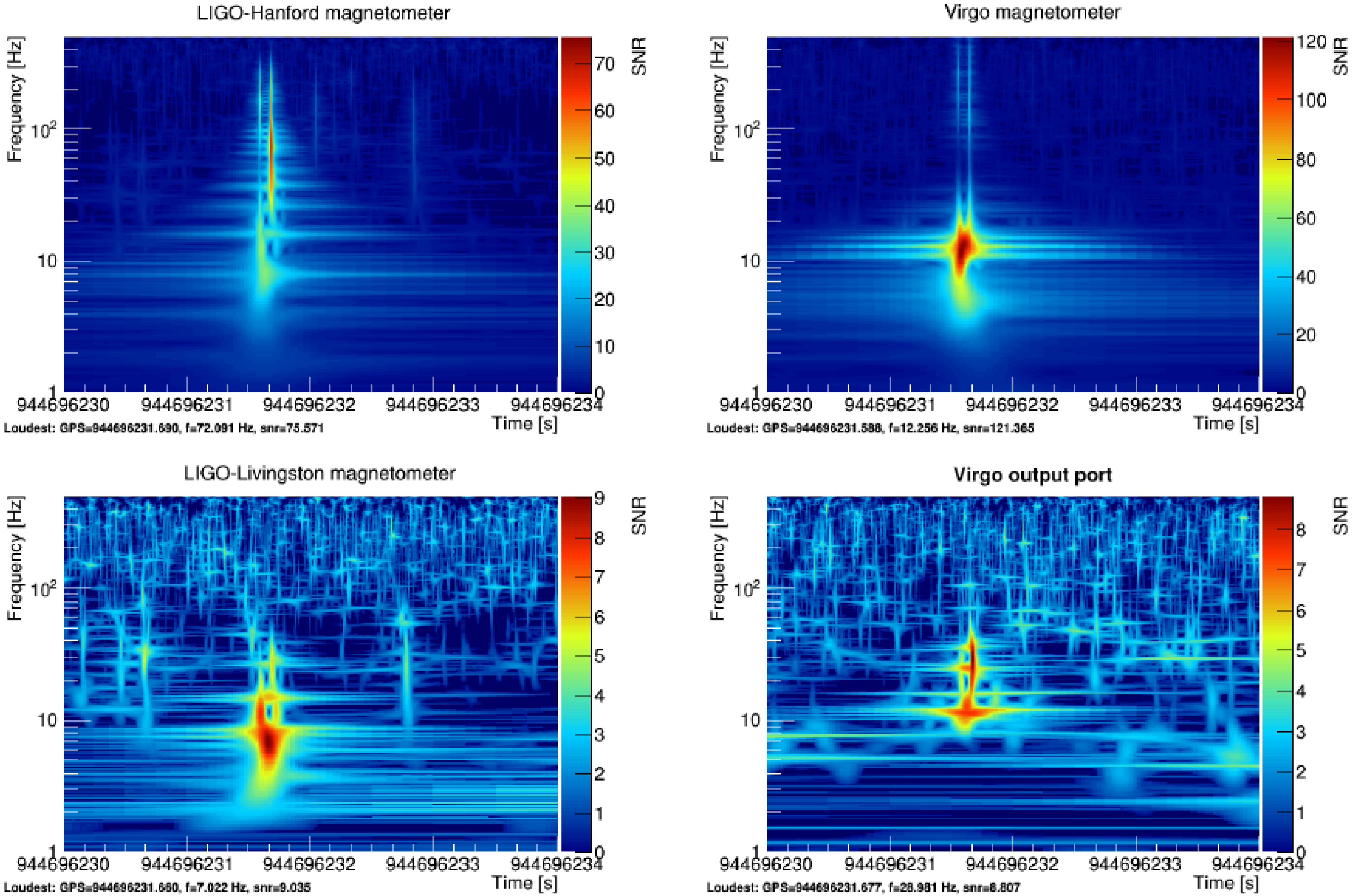

Time-frequency spectrograms of magnetometers located at the LIGO-Hanford, Virgo and LIGO-Livingston at the time of the December 12, 2009 positive Gigantic Jet at 23:36:56.55 UTC. The signal is clearly present in the magnetometers. Bottom right spectrogram shows the event in the Virgo gravitational-wave strain, h(t), data.

Correlated Transient Magnetic Noise – Time Slide Study For Coincident Events

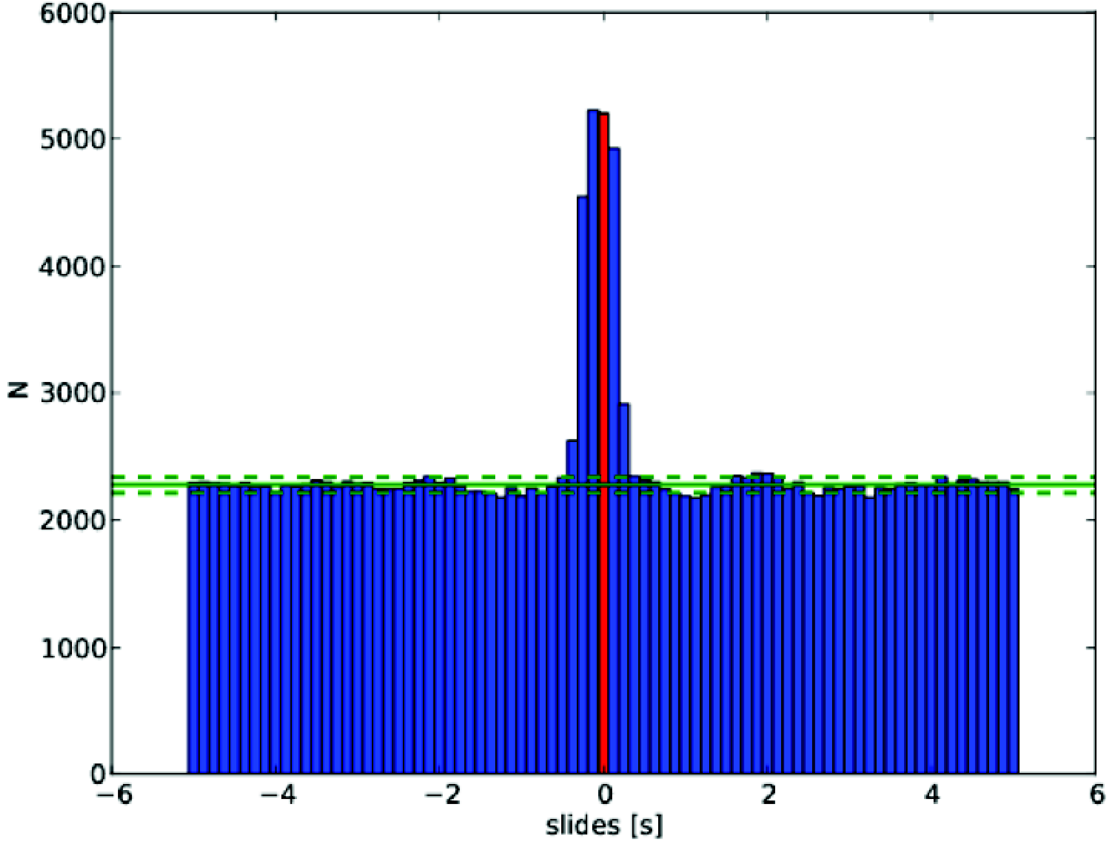

The number of coincident triggers as a function of time delay for magnetometers located at LIGO-Hanford and Virgo. The horizontal line represents the mean value of the time slide results (excluding the 0.625 s covered by the central 5 bins), while the dashed lines represent the standard deviation (again excluding the central 5 bins).

I. Kowalska et al., Classical and Quantum Gravity, Vol. 34, 074002 (2017)

Correlated Transient Magnetic Noise – The Source of the Schumann Resonances

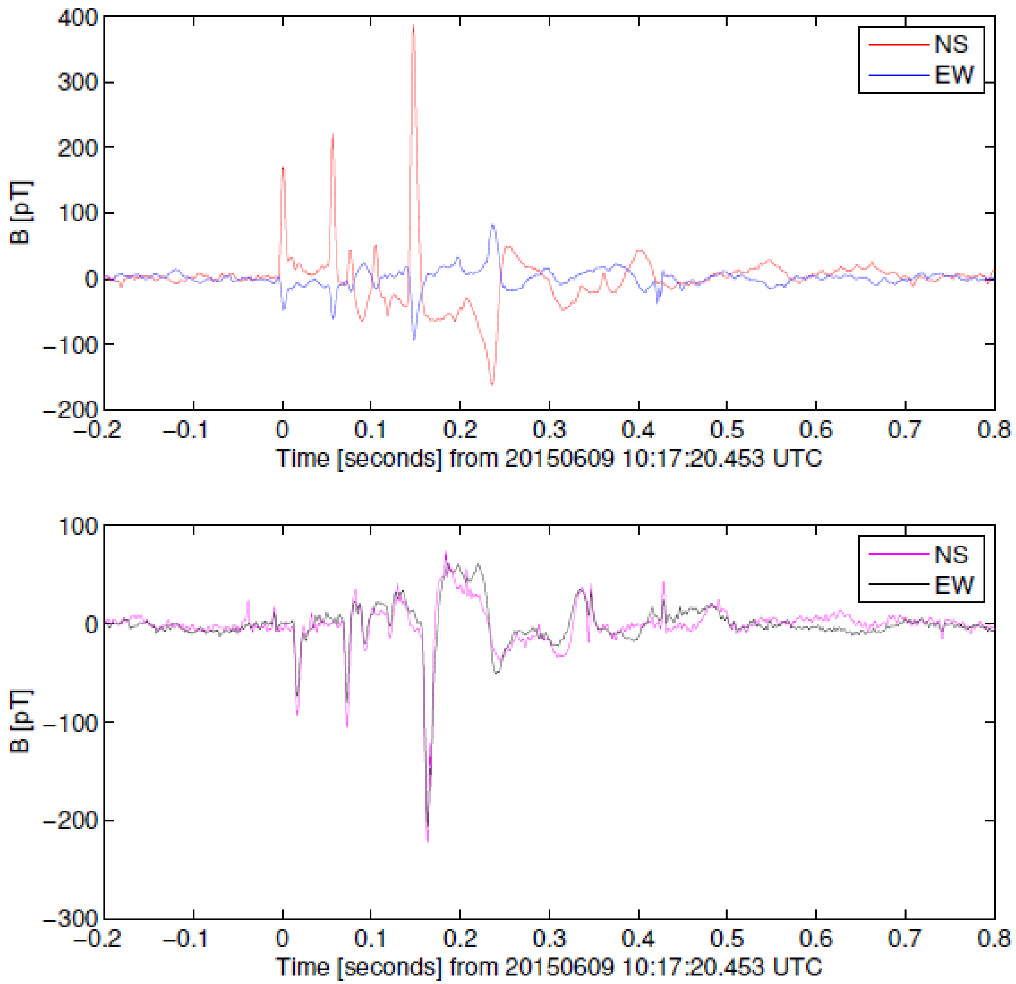

Example: lightning strike in China. 149 kA.

Observed in Poland (top) and Colorado (bottom).

50 to 100 large lightning strikes per second around the Earth.

2 to 3 coincident events per day with B > 200 pT

O1 analysis – verified that Schumann background did not contaminate results.

I. Kowalska et al., Classical and Quantum Gravity, Vol. 34, 074002 (2017)

Constraints on Cosmic String Parameters Coming from O1 Stochastic and Burst Search Results

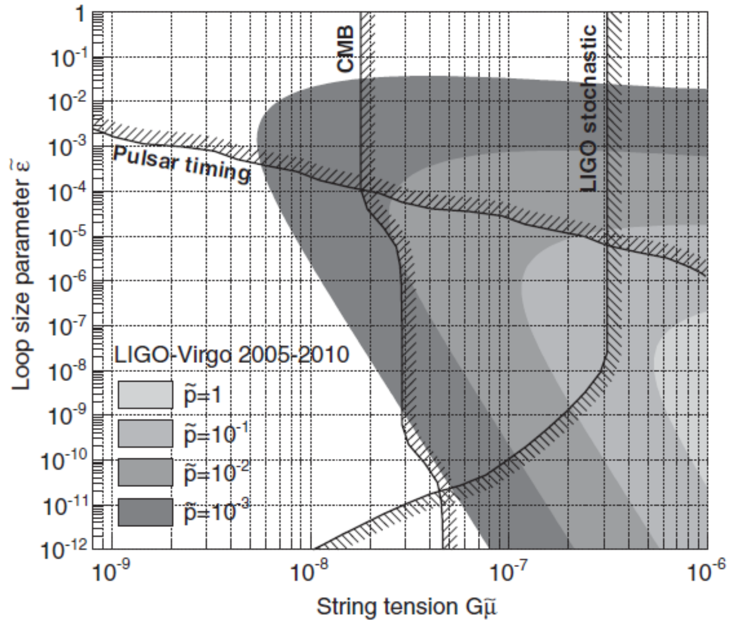

FIG. 2. Constraints on the modified cosmic string parameters $G\tilde{\mu} = g_1 g_2^{-2/3} G\mu$, $\tilde{\varepsilon} = g_1^{-1} g_2^{5/3} \varepsilon$, and $\tilde{p} = (n_c g_1)^{-1} g_2^{-1/3} p$, where g_1, g_2 and n_c are numerical factors of $\mathcal{O}(1)$. The gray regions, in different shades for four reconnection probability values, are rejected by our analysis at a 90% level. The black lines show the bounds derived from the GW stochastic background spectrum for $\tilde{p} = 10^{-3}$ and for a small loop scenario (CMB, pulsar, and LIGO data). The rejected region is always on the right-hand side of these lines.

Initial LIGO-Virgo results, PRL **112**, 131101 (2014)

Test of General Relativity with the Stochastic Gravitational-wave Background

A new search. Using Advanced LIGO O1 (and future) data to search for 6 polarizations. Non-GR. New search pipeline. Theoretical work on-going in parallel.

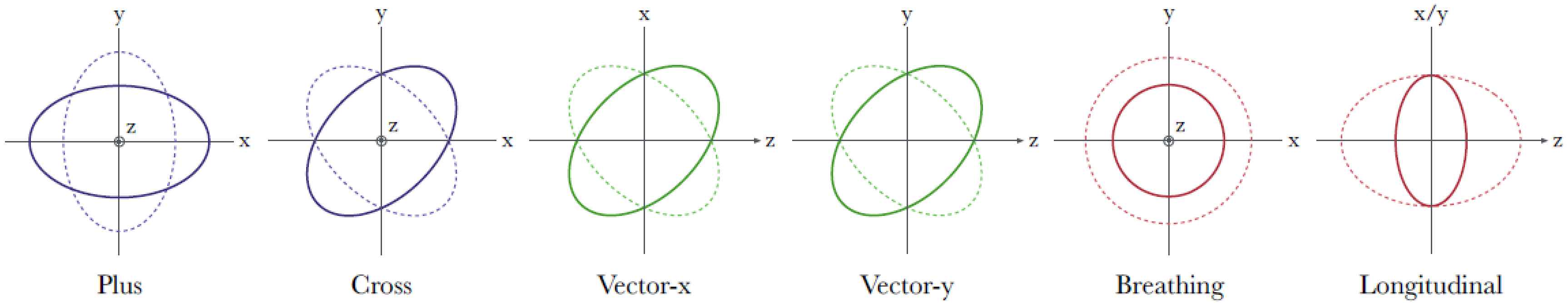

FIG. 1. Deformation of a ring of test particles under the six gravitational wave polarizations allowed in general metric theories of gravity. Each wave is assumed to propagate in the z-direction. While General Relativity allows only for two tensor polarizations (Plus and Cross), alternate theories allow for two vector (X and Y) and/or two scalar (Breathing and Longitudinal) polarization modes.

T. Callister, et al., arXiv:1704.08373

Test of General Relativity with the Stochastic Gravitational-wave Background

To come: results for a search for scalar, vector and tensort polarizations with O1 data.

A fully Bayesian (nested sampling) parameter estimation method will assign upper limits for energy of the different polarizations. Constraints will be placed on various non-GR theories.

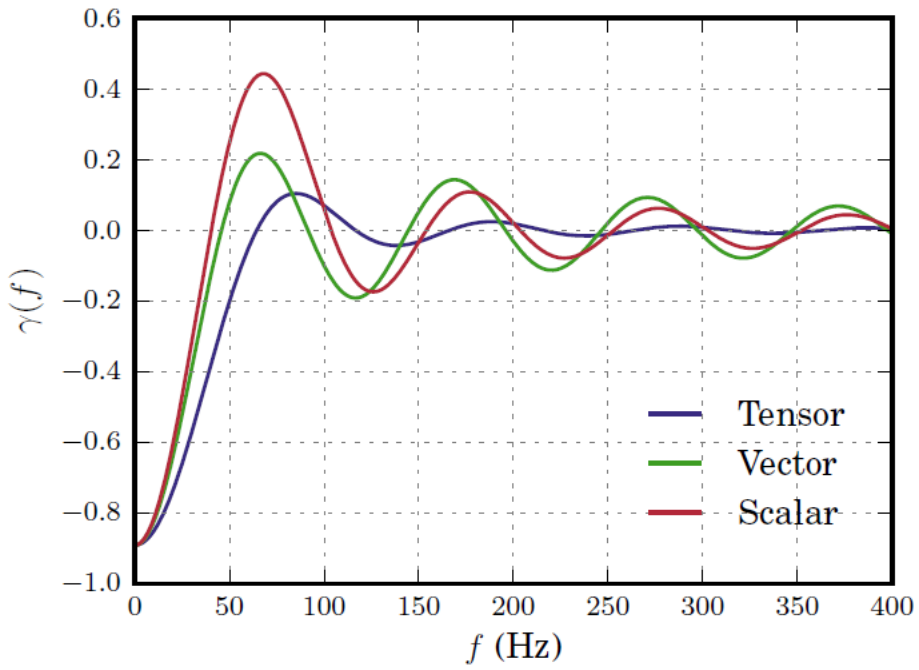

FIG. 2. Overlap reduction functions quantifying Advanced LIGO's sensitivity to isotropic backgrounds of tensor, vector, and scalar-polarized gravitational wave backgrounds.

arXiv:1704.08373

Test of General Relativity with the Stochastic Gravitational-wave Background

Projected sensitivity of Advanced LIGO to SGWBs of tensor, vector, and scalar radiation (solid blue, green, and red, respectively).

The limits that Advanced LIGO can place on flat vector and scalar-polarized backgrounds will therefore be similar to those placed on a flat tensorial background.

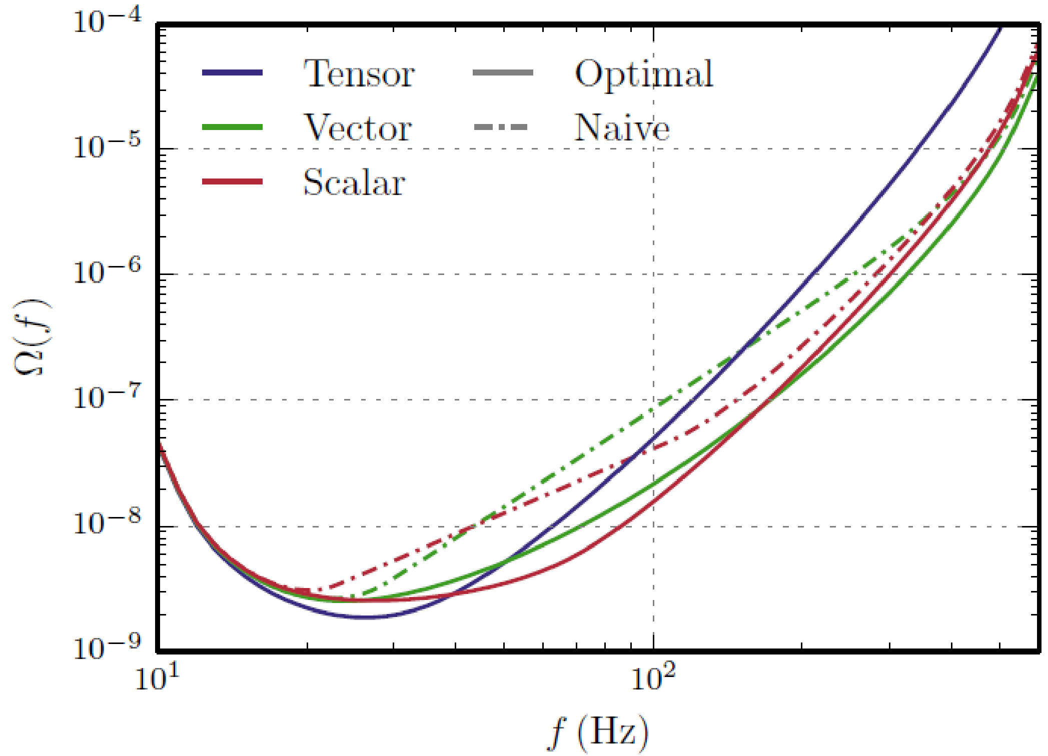

Advanced LIGO can place constraints on positively-sloped vector and scalar backgrounds that are up to an order of magnitude more stringent than those that can be placed on similarly-shaped tensor backgrounds.

Ability to resolve different polarizations will get better with Virgo, KAGRA,LIGO-India.

arXiv:1704.08373

Future Observing Runs

Living Rev. Relativity, **19**, (2016), 1
DOI 10.1007/lrr-2016-1

LIVING REVIEWS *in relativity*

Prospects for Observing and Localizing Gravitational-Wave Transients with Advanced LIGO and Advanced Virgo

Abbott, B. P. et al.
The LIGO Scientific Collaboration and the Virgo Collaboration
(The full author list and affiliations are given at the end of paper.)
email: lsc-spokesperson@ligo.org, virgo-spokesperson@ego-gw.it

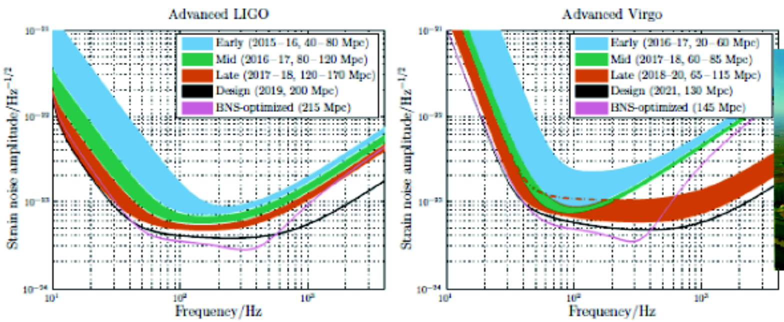

Figure 1: aLIGO (*left*) and AdV (*right*) target strain sensitivity as a function of frequency. The binary neutron-star (BNS) range, the average distance to which these signals could be detected, is given in megaparsec. Current notions of the progression of sensitivity are given for early, mid and late commissioning phases, as well as the final design sensitivity target and the BNS-optimized sensitivity. While both dates and sensitivity curves are subject to change, the overall progression represents our best current estimates.

2015 – 2016 (O1) A four-month run (beginning 18 September 2015 and ending 12 January 2016) with the two-detector H1L1 network at early aLIGO sensitivity (40 – 80 Mpc BNS range).

2016 – 2017 (O2) A six-month run with H1L1 at 80 – 120 Mpc and V1 at 20 – 60 Mpc.

2017 – 2018 (O3) A nine-month run with H1L1 at 120 – 170 Mpc and V1 at 60 – 85 Mpc.

2019+ Three-detector network with H1L1 at full sensitivity of 200 Mpc and V1 at 65 – 115 Mpc.

Living Reviews in Relativity **19**, 1 (2016)

LIGO Observing Run O2 ongoing

O2 Stochastic Update

- O2 sensitivity comparable to O1
- Many (but not all) noise lines have been cleaned up via commissioning
- O2 will probably have more that 2-times the O1 H1-L1 data
- Combined O1-O2 analysis, you can do the math: $\Omega_{GW} \propto 1/\sqrt{T}$
- Inclusion of Virgo in O2 not likely to change isotropic limit, but could have important implications for the directional searches.
- With Virgo, three detector combinations, and improved sky resolution.

LIGO-Virgo Summary/Conclusion

- The GW stochastic background from BBHs is expected to be in the higher end of previous predictions
- The background may be measured by LIGO/Virgo operating at or near design sensitivity.
- No evidence for a stochastic background in O1.
- Upper limit on a flat spectrum 33x better than with initial LIGO/Virgo
- O1 and O2 data will be analyzed together → more observation time

Extra Slides

Noise Lines In LIGO O1 Data

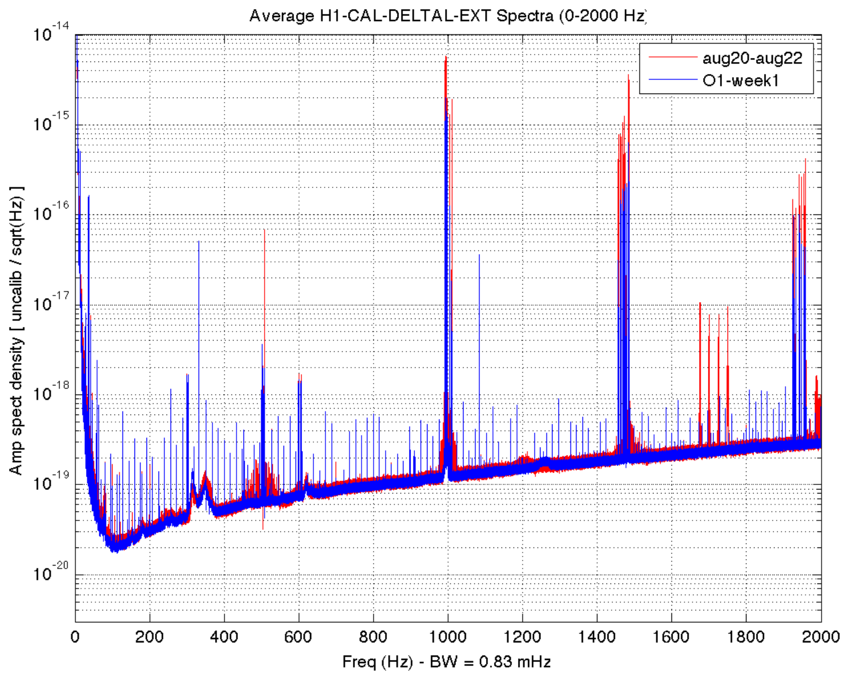

Noise Power Spectral Density H1 in O1

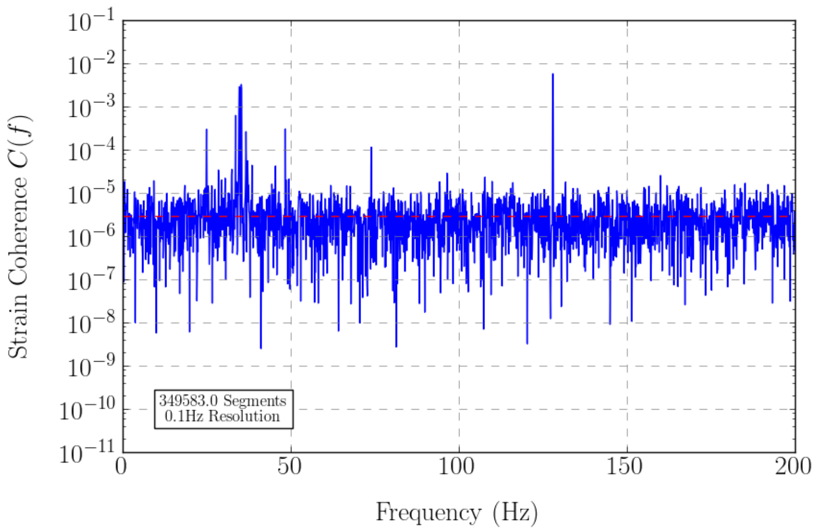

H1-L1 O1 Coherence

Common noise – similar equipment.
Bin size switched to 1/32 Hz for notching; nominally 0.25 Hz.

O1 Sensitivity to $\Omega_{gw}(f)$ Through the Observing Run

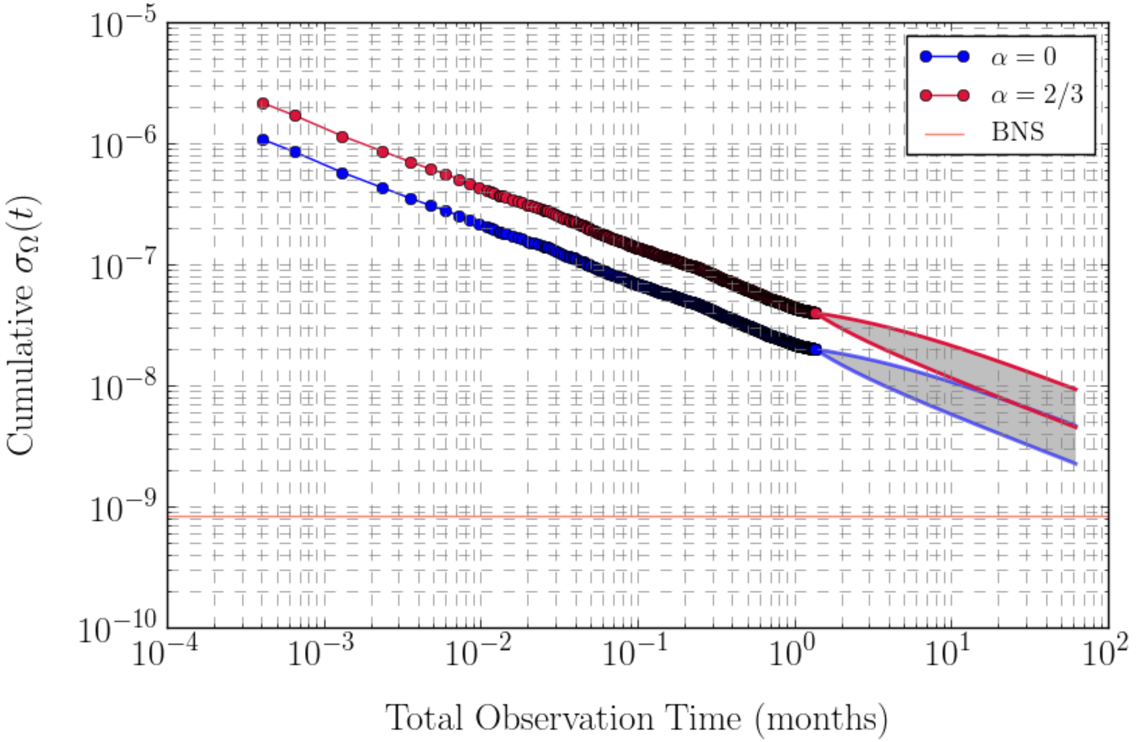

Integrated broadband search sensitivity σ(t) and 5 year predicted sensitivity vs cumulative observation time for a flat spectrum (α=0, blue) and for an astrophysical spectrum (α=2/3, red). The solid lines show the predicted future evolution of σ, achieved by extrapolating using the mean hourly sensitivity (upper bounds) and the best hourly sensitivity (lower bounds). The orange line represents the astrophysical prediction for the BBH/BNS background at 100Hz.

Advanced LIGO – Advanced Virgo

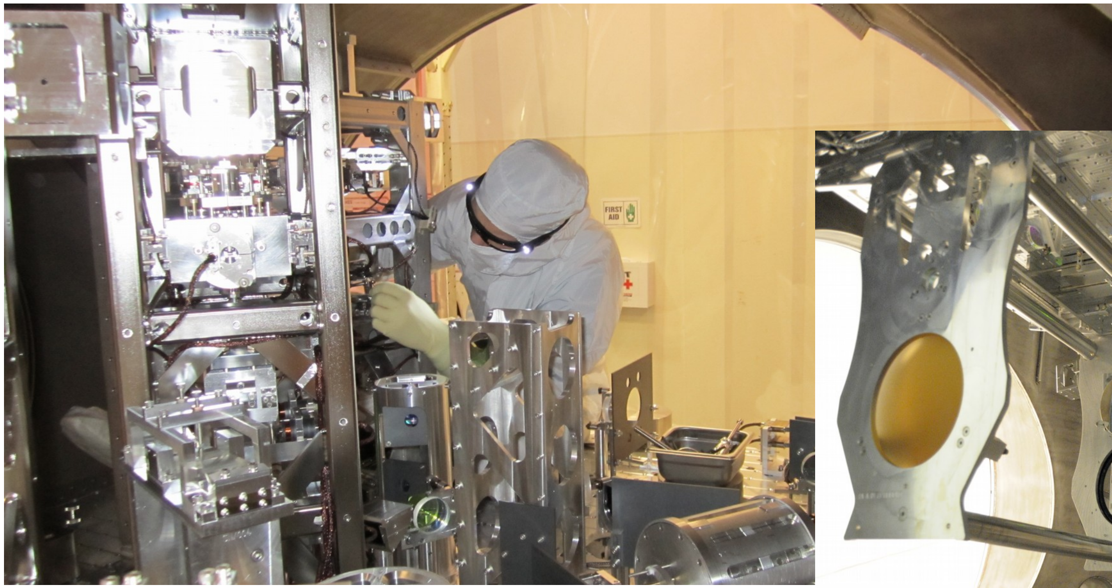

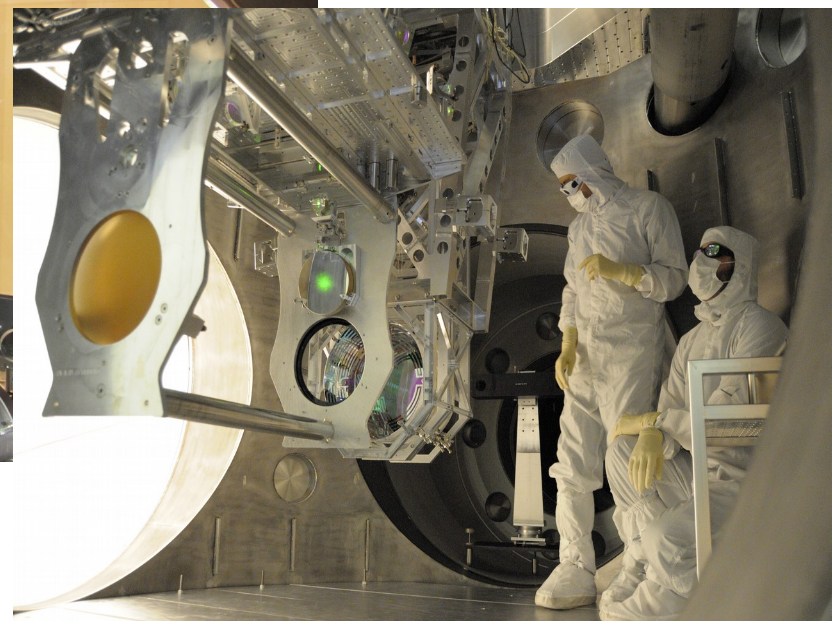

Built on the experience gained from the first generation (2004 - 2010) detectors

Built on the experience gained from the first generation detectors

Advanced LIGO

- Initial LIGO: 2005-2010.
- Advanced LIGO commissioned 2010-2015.
  - » Increased laser power
  - » Sophisticated seismic/vibration suppression
  - » Quadruple pendula suspensions
  - » Larger mirrors, better suspension material
  - » More complex and versatile interferometer configuration.

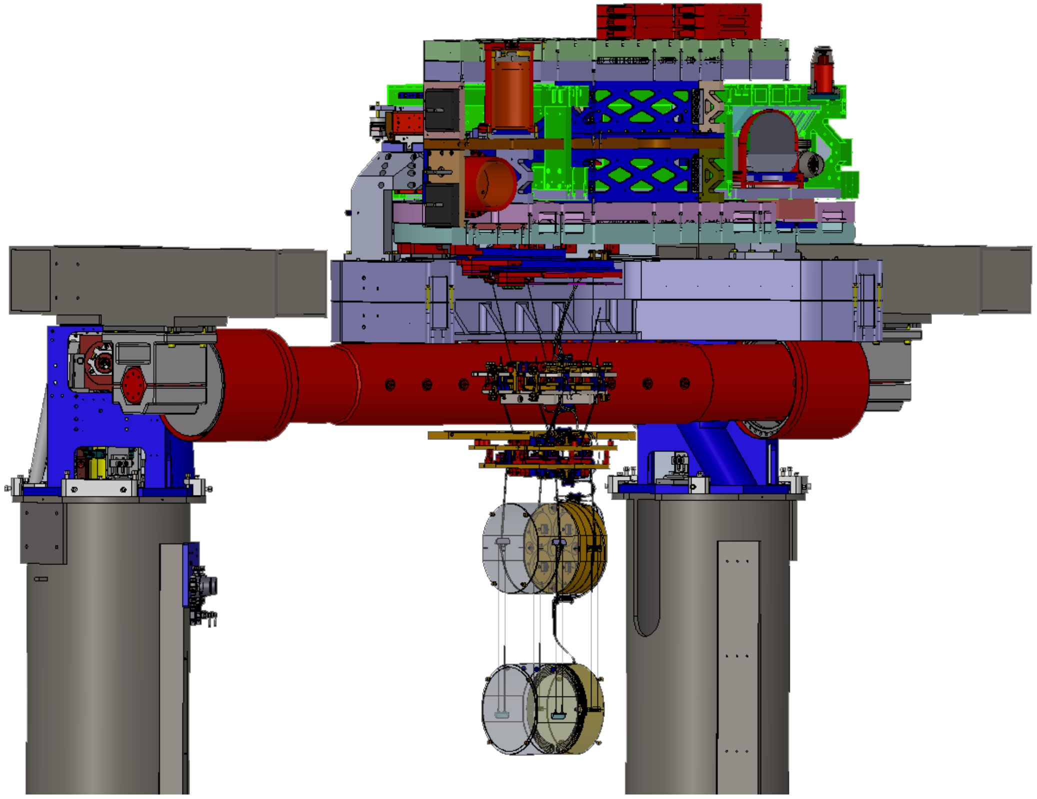

O2, second observing run, started last fall, goes to August.

Advanced Virgo

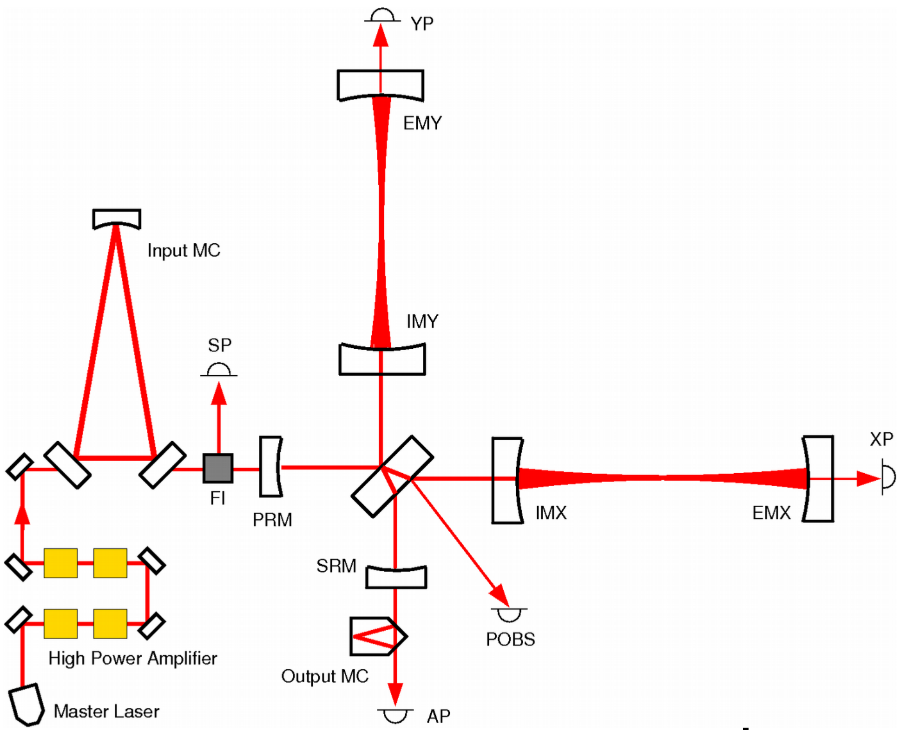

- Larger mirrors; better optical quality.
- Higher finesse of the arm cavities
- Increased laser power.
- Coming on-line in Spring 2017 to join O2.

Black Hole Population

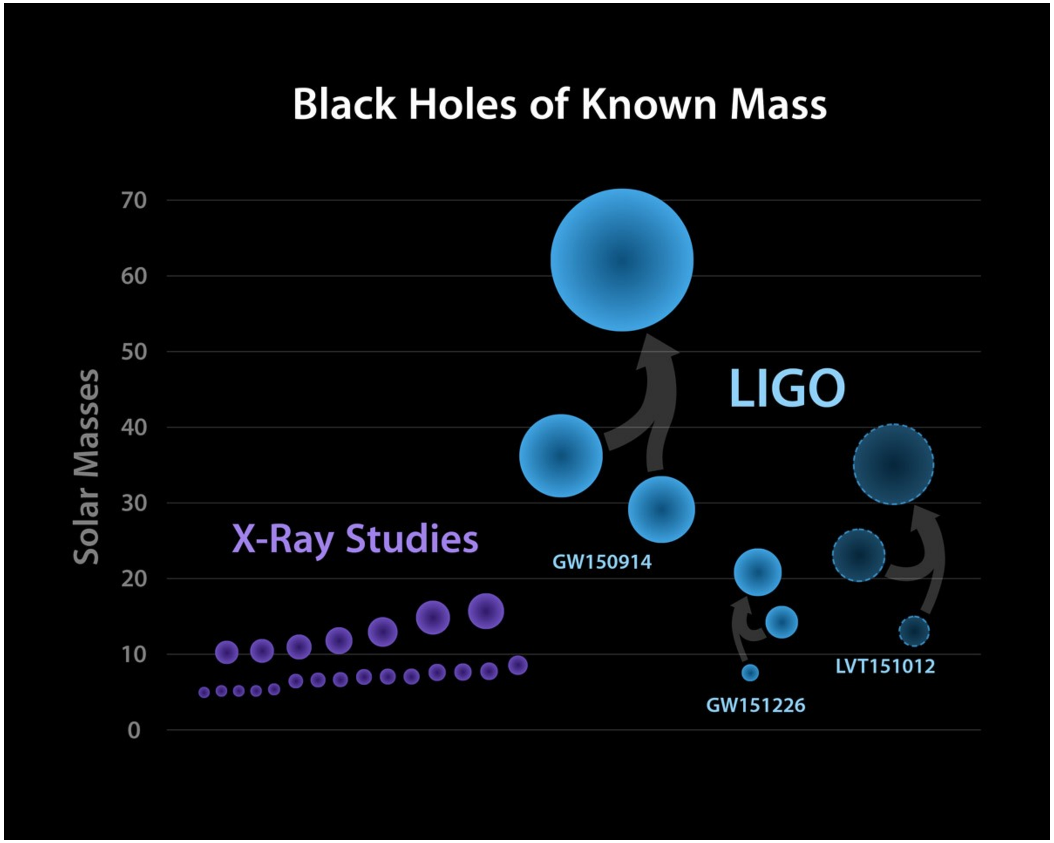

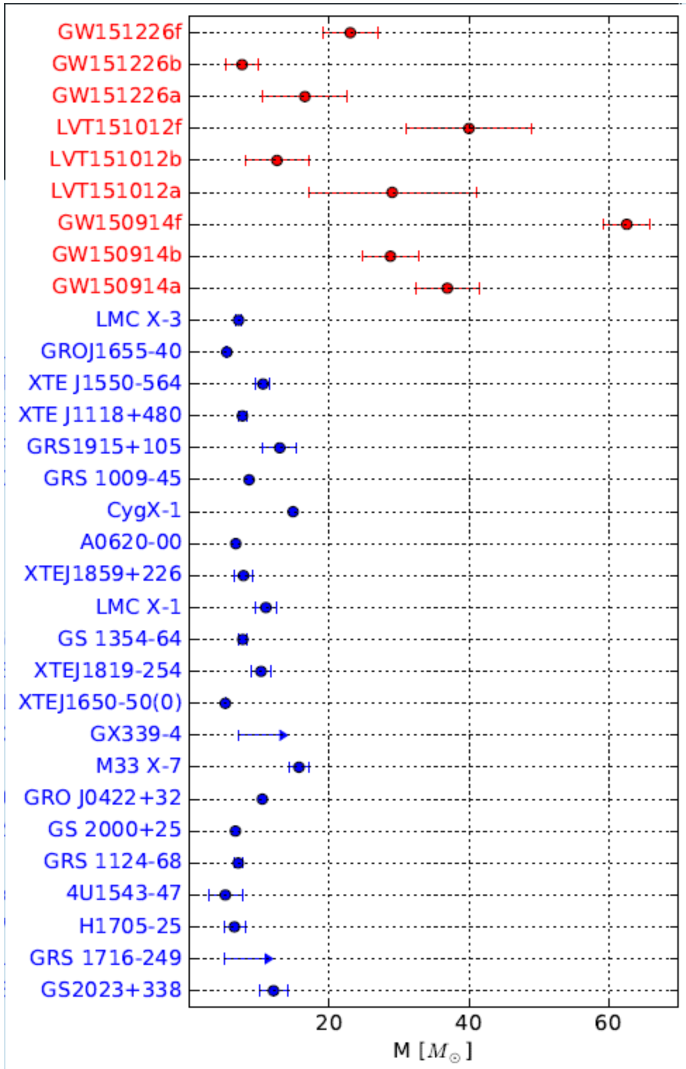

Image Credit LIGO

Binary Black Hole Merger Rate

- Assuming that all binaries are like these 3 events is not realistic.
- Try two alternative models:
  - Flat distribution in log m1 – log m2
  - (m1) $\propto m_1^{-2.35}$ with a uniform distribution for the second mass.
- Significantly different rate estimates.
- Altogether: 9 – 240 $\mathrm{Gpc}^{-3}\ \mathrm{yr}^{-1}$.
- Lower limit comes from the flat in log mass population and the upper limit from the power law population distribution.

- Rules out <9 $\mathrm{Gpc}^{-3}\ \mathrm{yr}^{-1}$, which were previously allowed.

Stochastic Gravitational-wave Background

A stochastic background of gravitational waves results from the superposition of a large number of independent unresolved sources at different stages in the evolution of the Universe.

- **Cosmological:** signature of the early Universe near the Big Bang *inflation, cosmic strings, phase transitions…*
- **Astrophysical:** since the beginning of stellar activity : *compact binary coalescences, core-collapse supernovas, rotating neutron stars, capture by SMBHs…*
- **What do we try to measure?**

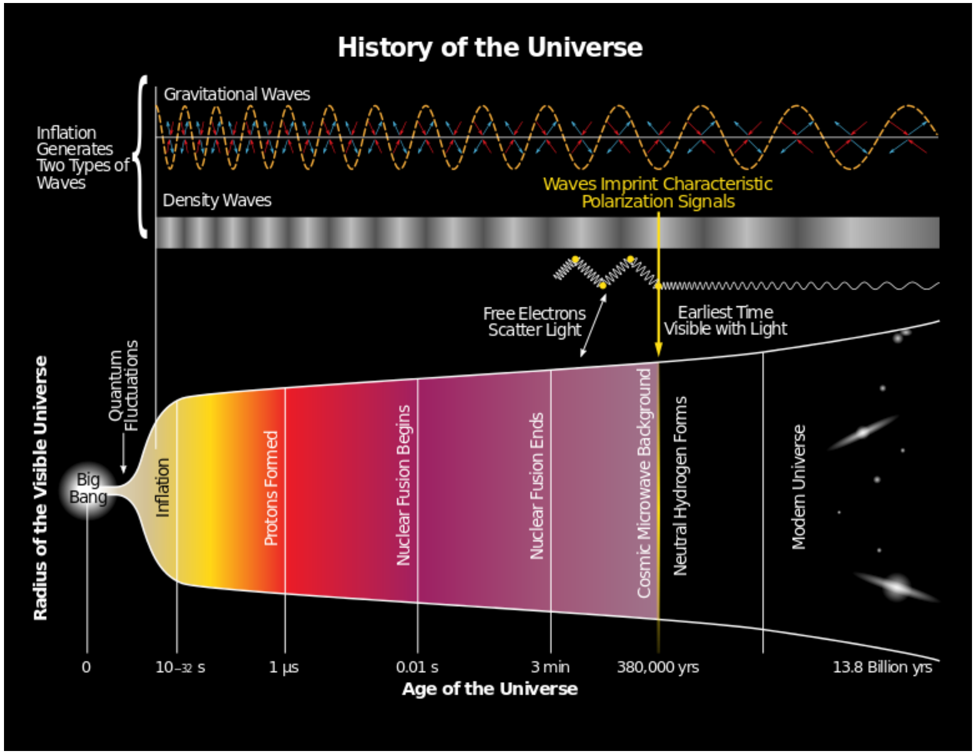

$$\Omega_{GW}(f) = \frac{f}{\rho_c}\frac{d\rho_{GW}}{df} \qquad \Omega_{GW}(f) = A(f/f_{ref})^{\alpha}$$